Artículo aceptado en / *Paper accepted in*

REVISTA MEXICANA DE CIENCIAS GEOLÓGICAS

Versión preliminar / *Draft versión*

Geology and geochronology of the Magdalena-Madera metamorphic core complex lower plate in the sierras Las Jarillas-El Potrero, northern Sonora

por / *by*

Teresita Sánchez Navarro, Michelle Vázquez Salazar, Carlos M. González-León, Luigi A. Solari, Anne E. Egger, Teresa Orozco-Esquivel, Margarita López-Martínez, Jonathan A. Nourse, Ofelia Pérez Arvizu, and Rufino Lozano-Santacruz

Artículo recibido: agosto 12, 2024
Artículo corregido recibido: abril 25, 2025
Artículo aceptado: abril 29, 2025
Versión preliminar publicada: mayo 1, 2025

Geology and geochronology of the Magdalena-Madera metamorphic core complex lower plate in the sierras Las Jarillas-El Potrero, northern Sonora

Teresita Sánchez Navarro[1], Michelle Vázquez Salazar[2], Carlos M. González-León[3], Luigi A. Solari[4], Anne E. Egger[5], Teresa Orozco-Esquivel[4], Margarita López-Martínez[6], Jonathan A. Nourse[7], Ofelia Pérez Arvizu[4], and Rufino Lozano-Santacruz[8]

[1]Posgrado en Ciencias de la Tierra, Estación Regional del Noroeste, Instituto de Geología, Universidad Nacional Autónoma de México, L.D. Colosio y Madrid, Hermosillo, México 83000.

[2]Ingeniería en Geociencias, Universidad Estatal de Sonora, Hermosillo, México 83100.

[3]Estación Regional del Noroeste, Instituto de Geología, Universidad Nacional Autónoma de México, L.D. Colosio y Madrid, Hermosillo, México 83000.

[4]Instituto de Geociencias, Universidad Nacional Autónoma de México, Juriquilla, Qro, México.

[5]Geological Sciences and Science Education, Central Washington University, 400 E. University Way, Ellensburg, WA 98926-7418.

[6]Departamento de Geología, Centro de Investigación Científica y de Educación Superior de Ensenada (CICESE), Carretera Ensenada-Tijuana 3918, Zona Playitas, Ensenada, México. (retired).

[7]Department of Geological Science, California State Polytechnic University, Pomona, 3801 West Temple Ave, Pomona, CA, 91768, USA.

[8]Universidad Nacional Autónoma de México, Instituto de Geología, Laboratorio Nacional de Geoquímica y Mineralogía, Ciudad Universitaria, Ciudad de México, 04510, México.

**Corrresponding author (C. M. González-León): cmgleon@unam.mx*

ABSTRACT

The area of sierras Las Jarillas-El Potrero in northern Sonora is interpreted as a portion of the lower plate of the Magdalena metamorphic core complex. Rock units that characterize this locality range in age from Jurassic to Eocene. Jurassic units comprise a small area of metasedimentary rocks that is probably correlative with the regional Middle Jurassic La Jojoba metasandstone, and is intruded by the La Cebolla granite of 158.1 ± 1 Ma (U-Pb, zircon). A younger succession consists from base upwards of a lower metasedimentary unit, a metalimestone unit, and an upper metasedimentary unit. The lower and upper units have similar lithologies of metapelites, metasandstones, and metavolcanic rocks for which maximum depositional ages (U-Pb, zircon) of ca. 119 to ca. 112 Ma were obtained. The intermediate unit consists

of recrystallized limestone with interbedded metapelite and metasandstone. These three units that probably correlate with nearby unmetamorphosed outcrops of the Bisbee Group are intruded by the two-mica and garnet leucocratic mylonitic granites Las Jarillas, dated at 60.1 ± 0.9 Ma (MSWD= 7), and La Yegua, dated at 46.9 ± 0.3 Ma (MSWD= 0.8) (U-Pb, zircon). At the outcrop scale, Las Jarillas granite is fine-grained and saccaroid, whereas the La Yegua granite is medium- to coarse-grained, with common pegmatitic zones and abundant xenoliths of quartzo-feldspathic schists.

Mylonitic foliation in the area predominantly strikes NNW-SSE and dips gently NE and SW, with a NE65°SW trending lineation and average plunge of 16° NE and SW. The mylonitic granites record ductile to brittle-ductile deformation with foliation defined by bands of dynamically recrystallized quartz that envelop feldspar porphyroclasts. The metasedimentary and metavolcanic rocks show continuous and/or spaced cleavage defined by alignments of muscovite, biotite and epidote and subordinate tourmaline, titanite, garnet, hornblende, staurolite, actinolite, zoisite, and opaque minerals. These minerals suggest upper greenschist to lower amphibolite facies metamorphism for the rocks in the area. Mica-fish and S-C foliation kinematic indicators consistently indicate a top-to-the-SW tectonic transport direction. A concentrate of muscovite and quartz from a metasandstone sample yielded a cooling age of 24.14 ± 0.57 Ma ($^{40}Ar/^{39}Ar$), similar to muscovite ages reported by Wong et al. (2010) for the nearby Magdalena-Madera metamorphic core complex. We consider Sierras Las Jarillas-El Potrero to be part of the Magdalena-Madera complex that was exhumed in the footwall of the regional Magdalena-Tubutama detachment fault, which is inferred to pass directly southwest of the study area. A secondary, west-dipping detachment fault in the study area separates the Jurassic and Lower Cretaceous footwall successions near Cerro Picacho. The identified Jurassic through Eocene units, structural overprint, and new geochronologic results are consistent with large-magnitude late Oligocene-early Miocene extension that has affected the region.

Keywords: Magdalena-Madera metamorphic core complex, U-Pb geochronology, $^{40}Ar/^{39}Ar$ thermochronology, Cenozoic, Sonora.

RESUMEN

El área de las sierras Las Jarrillas-El Potrero, norte de Sonora, se interpreta como parte de la placa inferior del complejo de núcleo metamórfico Magdalena-Madera. En el área afloran rocas que van del Jurásico al Eoceno. De las rocas jurásicas se tiene un afloramiento pequeño de metasedimentos asignado

tentativamente a la unidad regional metaarenisca La Jojoba, el cual está cortado por el granito La Cebolla de 158.1±1 Ma (U-Pb, circón). También se reconoce una sucesión metasedimentaria asignada a la unidad metasedimentaria inferior, unidad de metacalizas y a la unidad metasedimentaria superior. Las litologías de las unidades inferior y superior corresponden a metapelitas, meta-areniscas y rocas metavolcánicas de las que se obtuvieron edades máximas de depósito (U-Pb, circón) entre ca. 119 y ca. 112 Ma. La unidad intermedia consiste principalmente de calizas recristalizadas que se alternan con metapelitas y meta-areniscas. Estas unidades se correlacionan con formaciones no metamofoseadas del Grupo Bisbee y están intrusionadas por los granitos miloníticos Las Jarillas, fechado (U-Pb, circón) en 60.1±0.9 Ma (MSWD= 7) y La Yegua de 46.9 ± 0.3 Ma (MSWD= 0.8). Estos son granitos leucocráticos, de dos micas y granate que en afloramiento se distinguen por ser de grano fino y sacaroide el primero, y de grano medio a grueso, con zonas pegmatíticas y abundantes xenolitos de esquistos cuarzo-feldespáticos el segundo.

Las rocas del área presentan foliación milonítica con orientación predominante hacia el NNW-SSE con echados de bajo ángulo hacia el NE y SW, y lineación promedio de NE65°SW con buzamiento promedio de 16° en ambas direcciones. Los granitos miloníticos tienen marcada deformación dúctil, a frágil-dúctil con foliación definida por bandas de agregados de cuarzo recristalizado que envuelven a porfidoclastos de feldespatos. Las rocas metasedimentarias y metavolcánicas muestran clivaje continuo y/o espaciado, definido por el alineamiento de moscovita, biotita y epidota y en menor proporción por turmalina, titanita, granate, hornblenda, estaurolita, actinolita, zoisita y minerales opacos. Esta asociación mineral sugiere un grado de metamorfismo de facies de esquistos verdes a anfibolita. Indicadores cinemáticos obtenidos sobre todo de "mica-fish" y foliación S-C, indican consistentemente un sentido de cizallamiento de la cima hacia el SW, por lo que se infiere que una falla de despegue está situada al sur del área de estudio. Una edad $^{40}Ar/^{39}Ar$ obtenida de una mezcla de moscovita y cuarzo separadas de una metaarenisca del área dio una edad de enfriamiento de 24.14 ± 0.57 Ma, la cual es similar a edades obtenidas en moscovita por Wong et al. (2010) para el vecino complejo de núcleo metamórfico Magdalena-Madera. Consideramos que el área de las sierras Las Jarillas-El Potrero es parte de ese complejo y que la falla de despegue Magdalena-Tubutama que lo exhumó pasa directamente al suroeste del área de estudio. Una falla secundaria de este tipo que separa a rocas jurásicas y cretácicas se tiene en el Cerro El Picacho de la Sierra El Potrero. Las litologías con edades del Jurásico al Eoceno, las estructuras que las afectan y las edades geocronológicas obtenidas son consistentes con la extensión de gran magnitud que afectó a esta región del Oligoceno tardío al Mioceno temprano.

Palabras clave: Complejo de núcleo metamórfico Magdalena-Madera, geocronología U-Pb, Termocronología $^{40}Ar/^{39}Ar$, Cenozoico, Sonora

INTRODUCTION

The physiographic and tectonic extensional Basin and Range province (BRP) of western North America is characterized by NNW-SSE-oriented horsts and grabens that were formed during late Tertiary high-angle normal faulting. In regions of greater extension within this province, the strain occurred on low-angle normal faults (detachment faults), that exhumed rocks of deeper parts of the crust to form metamorphic core complexes (MCCs) (Wernicke, 1992).

Wernicke (1992) recognized northern, central, and southern subprovinces within the BRP and included the region of Arizona and Mexico in the southern subprovince (Figure 1). Although the extensional event that produced these subprovinces was diachronous (Dickinson, 2002), Wernicke (1992) suggested that for the central and southern subprovinces, extension and magmatism occurred through an initial stage of low rate extension with formation of intermountain basins followed by silicic volcanism, a second stage of high magnitude crustal extension and associated silicic volcanism, and a later stage of waning extension accompanied by basaltic to bimodal volcanism.

The BRP evolved since the Eocene, after the western region of North America was affected by the Sevier and Laramide compressive orogenies which produced thickening of the continental crust from the Cretaceous to the Paleogene (Coney and Harms, 1984). Several authors favored the idea that the crustal thickening produced a gravitational instability that later facilitated the extension of the continental crust to develop the BRP (Coney and Harms, 1984; Dickinson, 1991; Wernicke, 1992), although other factors that may have contributed to the extensional process are crustal weakening produced by the prolonged thermal effect of Laramide magmatism (Whitney et al., 2013).

Tectonic extension and magmatism in the southern BRP is proposed to have occurred concomitant to steepening of the subduction angle of the Farallon plate and its retreat to the trench by slab rollback during late Eocene to Miocene time (Dickinson, 1991). According to Dickinson (1991), during the slab rollback event, the previously thickened Laramide crust of southwestern North America initially underwent a large-scale extensional phase produced by low-angle faulting that exhumed rocks in the MCCs, which was followed by the high-angle block faulting of the BRP. In northwestern Mexico, extension associated with the BRP began at ~30 Ma, shortly after the beginning of the most important

magmatic pulse between ~34 and 18 Ma that formed the Sierra Madre Occidental volcanic province (Bryan and Ferrari, 2013; Ferrari et al., 2018).

The MCCs within the BRP formed in areas of large-magnitude extension and presently they define a discontinuous belt that extends from southwestern Canada to northwestern Mexico (Whitney et al., 2013). The MCCs are defined as dome or arcuate structures, composed of a lower plate composed by ductilely deformed rocks and associated intrusions that underlie a main, low-angle (detachment) fault that displaces rocks of the upper plate by tens of kilometers. The lower-plate rocks, that were exhumed from the middle crust (Davis, 1980; Davis, 1983; Davis et al., 1986; Platt et al., 2015), record characteristic features of dynamic metamorphism with the development of mylonitic fabrics produced at ductile, or ductile-brittle domains of deformation and at temperatures between 280 - 500°C (Passchier and Trouw, 2005). The upper plate rocks in most core complexes are affected by brittle deformation.

Metamorphic core complexes that extend from southeastern California to southern Arizona and northern Sonora (Figure 1) are considered to be located in a region having of the highest continental crustal extension. Those situated between the Chemehuevi and South Mountains complexes have a common direction of displacement of their upper plate, respect their lower plate, towards the northeast (Figure 1). The MCCs of southern Arizona include the Santa Catalina-Rincon, Picacho, Tortolita, Coyote and Pozo Verde mountains, and those in northern Sonora include the Tubutama, Magdalena-Madera, Sierra Aconchi, Puerta del Sol and Sierra Mazatán. They all have in common a dominant displacement direction of their upper plates towards the southwest (Nourse et al., 1994; Nourse, 1995; Spencer et al., 2019) (Figure 1).

Exhumation of the MCCs of southeastern California and central Arizona is broadly of Miocene age, with ages of syn-kinematic minerals that indicate initiation between 24 and 22 Ma and end of fault displacement at 18 Ma (Gottardi et al., 2020). The MCCs of southern Arizona are slightly older with onset of extension and cooling ages between ca. 30 and 18 Ma (Gottardi et al., 2020), whereas ages of the Sonora MCCs indicate that they were active between 25 and 15 Ma, according to different thermochronometric systems (Nourse et al., 1994; Vega Granillo and Calmus, 2003; Wong and Gans, 2008; Wong et al., 2010, Lugo Zazueta, 2006; González-Becuar et al., 2017; Almada Gutiérrez, 2020).

The present work reports on the geology of the Las Jarillas-El Potrero mountain ranges of northern Sonora (Figure 1) in order to compare its evolution with that of the adjacent Magdalena-Madera metamorphic core complex, of which Nourse (1989, 1995) proposed it is part. Our objective is to better

understand the geology, deformation and metamorphism, and the age of the rocks and events of this area that has not previously been studied in detailed. For this purpose, we conducted field mapping, collected structural data and samples for petrography, U-Pb and $^{40}Ar/^{39}Ar$ geochronology and for major and trace element geochemical analyses. The results help to partially advance in the understanding of the evolution of the Magdalena-Madera metamorphic core complex.

REGIONAL SETTING

Northern Sonora is characterized by a Paleoproterozoic basement of crystalline rocks, which is a continuation of the Mojave, Yavapai, and Mazatzal crustal provinces of the southwestern United States of America (see summary in Iriondo and Premo, 2011). Recognition of a juxtaposition between the basement rocks of the Mazatzal province with the Mojave and Yavapai crustal provinces of the Caborca block in northern Sonora (Figure 2), was one basis for introducing the hypotheses of the NW-SE-trending left-lateral Mojave-Sonora (Anderson and Silver, 1979) or California-Coahuila faults (Dickinson and Lawton, 2001; Lawton et al., 2017) (Figure 2) of proposed Middle to Late Jurassic, or late Paleozoic age, respectively, that translated the Caborca block located south of the fault, for more than 800 km from east central and southwestern California.

Outcrops of crystalline Precambrian rocks are relatively abundant in the Caborca block, but scarce and isolated in the Sonoran Mazatzal block to the north. The pre-Cretaceous cover of the Caborca block basement is made up of a Neoproterozoic to Lower Jurassic sedimentary succession and plutonic and volcanic rocks of Permo-Triassic and Jurassic magmatic arcs (Arvízu et al., 2009; Arvízu and Iriondo, 2015), whereas the pre-Cretaceous cover of the Mazatzal province consists of Cambrian to Permian strata in northeastern Sonora, and widespread volcanic and plutonic rocks of the Jurassic continental Cordilleran magmatic arc (Busby-Spera, 1988).

The Jurassic and older rocks of the Caborca and Mazatzal blocks are overlain by the siliciclastic and carbonate succession of the Bisbee Group, that accumulated from the Late Jurassic to the Early Cretaceous in the Bisbee Basin (Lawton et al., 2020) in northern Sonora. Disruption of the Bisbee Basin began in the early Late Cretaceous, at the onset of Laramide shortening, which produced syntectonic conglomerates of the Cocóspera and Altar formations and large volumes of arc magmatism (Damon et al., 1983; Roldán-Quintana, 1991; McDowell et al., 2001; Valencia-Moreno and Ortega-Rivera, 2011; Valencia-Moreno et al., 2021). The Laramide tectono-magmatic event produced regional crustal thickening (Chapman et al.,

2020) and local metamorphism in Sonora (Iriondo et al., 2005; González-Becuar et al., 2017; Jacobson et al., 2019) and neighboring areas of Arizona (Goodwin and Haxel, 1990; Haxel et al., 1984; Chapman et al., 2020).

The Basin and Range extensional event that followed, started in Sonora during the late Oligocene and extended into the middle Miocene (Stewart and Roldán-Quintana, 1994; McDowell et al., 1997; González-León et al., 2010) giving rise to NW-SE to NE-SW-oriented horst and grabens, and localized areas of deep crustal exhumation that formed a belt of MCCs from the US border in the north, to the Sierra Mazatán in central Sonora. Based on $^{40}Ar/^{39}Ar$ thermochronological studies, Wong et al. (2010) concluded that extension that gave rise to these MCCs began synchronously at approximately 25 Ma, and in most areas ended at ca.15 Ma.

Davis et al. (1981) first recognized the Sierra Mazatán core complex in central Sonora and the Magdalena-Madera, Altar, Tubutama, Sásabe and sierras Las Jarillas-El Potrero MCCs in northern Sonora (Figure 2). These authors also noted that northern Sonora core complexes were composed of sedimentary, volcanic and plutonic rocks of presumed Jurassic age, with low- to medium-grade metamorphism.

The Magdalena-Madera metamorphic core complex was studied in detail by Nourse (1989; 1990; 1995), who recognized the mylonitic units of the lower plate, the Magdalena-Tubutama detachment fault (Figure 2) that controlled it, and rocks of the upper plate. According to Nourse, rocks of the lower plate are Jurassic metarhyolite, metasandstone, and metaconglomerate intruded by granitic plutons of the Jurassic continental volcanic arc, and deformed sedimentary rocks of Cretaceous age that were affected by the emplacement of at least three generations of two-mica leucocratic granites and biotite granitoids of Late Cretaceous to Eocene age.

Nourse (1989) proposed that the lower-plate rocks of the MCCs of northern Sonora record shortening, regional metamorphism, and granitic plutonism associated with the Laramide orogeny, and a younger mylonitic deformation consisting of shallow SW-dipping foliation and N30° - 50°E lineations that plunge to the SW produced during the development of the Magdalena-Madera metamorphic core complex. Nourse (1989) estimated that the Magdalena-Tubutama detachment fault (Figure 2), along which the complex was exhumed, has a dip <30° and a SW displacement of 15 to 20 km. The upper plate consists mainly of sedimentary and volcanic rocks of the Magdalena Formation that was accumulated during the detachment displacement; outcrops of this unit are found near the town of same name. The age of deformation in the Magdalena-Madera metamorphic core complex is constrained by K-Ar ages between

ca. 27 Ma and 19 Ma obtained from volcanic rocks of the syntectonic Magdalena Formation (Miranda-Gasca and De Jong, 1992; Wong et al., 2010), and by $^{40}Ar/^{39}Ar$ thermochronology ages in K-feldspar and muscovite from mylonitic granites of the lower plate that indicate rapid extension and uplift between 25 Ma and 22 Ma, ending at 20 Ma (Wong et al., 2010).

Other Tertiary MCC lower plate areas with mylonitic fabrics were recognized by Nourse et al. (1994) between the Magdalena-Madera and Pozo Verde MCCs in northern Sonora; these include sierras Las Jarillas-El Potrero, El Álamo Viejo (Sánchez Navarro, 2018), Santa Teresa, Tubutama, San Juan, and cerro Carnero (Figure 2). Rocks of these areas consists of lineated metasedimentary rocks of greenschist facies, which are cut by mylonitic leucocratic granites, two-mica granites, and pegmatite dikes. In the cerro Carnero (Figure 2), Jacobson et al. (2019) reported a 21.2 ± 0.2 Ma U-Pb (SHRIMP-RG) crystallization age for the deformed Rancho Herradura granodiorite, and Hayama et al. (1984) dated the host Altar Schist at ca.17 to 15 Ma (K-Ar), while Jacobson et al. (2019) interpreted these as cooling ages associated with a detachment fault.

The Las Jarillas-El Potrero mountain ranges are located in the northern portion of the state of Sonora, 20 km northwest of the town of Santa Ana (Figures 1 and 2). These ranges represent a morphological unit of nearly N-S direction, 23 km long and 11 km wide. The rocks of this area were first assigned to the Precambrian by Salas (1968), who recognized mylonites, cataclasites and phyllonites with regional metamorphism of greenschist facies, and with local contact metamorphism. Later, Morales Montaño (1984) proposed that these rocks consist of mica schists, quartzites, marbles, quartz-feldspathic gneisses, calcic schists, and granitic intrusions that were deformed during the Middle to Late Jurassic.

Nourse (1994) considered the sierras Las Jarillas-El Potrero as a horst, bordered by inferred N-S normal faults and separated from the adjacent ranges by wide valleys. He reported that the rocks in the area consist of deformed metasediments cut by dikes and sills of two-mica leucocratic granites with mylonitic fabric, and with a mineral associations indicative of greenschist facies metamorphism. He tentatively correlated the metasedimentary rocks with Lower Cretaceous strata outcropping in neighboring areas, or with rocks of the regional Jurassic magmatic arc.

According to Jiménez García et al. (1999), rocks cropping out in the study area are metavolcanosedimentary rocks of presumed Early Jurassic age, of greenschist to amphibolite facies, that are intruded by mylonitic granitic plutons. In a more recent study, Vázquez Salazar (2018) named informally the Rancho Las Jarillas and Rancho La Tinaja units composed of metasedimentary and

metavolcanic rocks that were assigned to the Jurassic. Based on U-Pb zircon dating, this author also recognized the La Cebolla granite of Jurassic age, metasedimentary rocks that she correlated with the Bisbee Group, and the Las Jarillas and La Yegua granites of Paleogene age.

METHODS

Field mapping was conducted at a scale of 1:50,000 using the Santa Ana (H12A69) and El Carrizo (H12A59) topographic base maps (INEGI, 1975a, b), and the Santa Ana geological-mining map (H12-A69) published by Servicio Geológico Mexicano (Jiménez García et al., 1999). During fieldwork, lithostratigraphic units were recognized and data on stratification, foliation, lineations and axial planes were obtained. The structural data were interpreted with Stereonet 10 (Allmendinger, 2019). Representative rock samples were collected for petrographic analysis, and oriented samples were collected for identification of kinematic indicators. We also collected samples of granites, metasedimentary and metavolcanic rocks to obtain: (1) crystallization and maximum depositional ages by U - Pb dating of zircon, (2) $^{40}Ar/^{39}Ar$ thermochronology analysis in micas, and (3) geochemical analyses with the purpose of classifying the metavolcanic rocks.

The petrographic thin sections and the whole-rock sample preparations were carried out in the laboratories of the Estación Regional del Noroeste, Instituto de Geología, UNAM. The mineral separation, zircon mounting and dating were performed at the Laboratorio de Estudios Isotópicos, Instituto de Geociencias, UNAM. U-Pb analyses were performed by laser ablation-inductively coupled plasma-mass spectrometry (LA-ICP-MS) according to the methodology described by Solari et al. (2018). Rock samples for $^{40}Ar/^{39}Ar$ geochronological analyses were processed at the Laboratorio Interinstitucional de Geocronología de Argón (LIGAr), Instituto de Geociencias, UNAM and Laboratorio de Geocronología, CICESE. Geochemical analyses of major oxides were conducted in Laboratorio Nacional de Geoquímica y Mineralogía (LANGEM) of the UNAM and the trace element contents were determined by inductively coupled plasma mass spectrometry (ICP-MS) at the Instituto de Geociencias, UNAM, following procedures referred in González-León et al. (2021).

RESULTS

Lithologic units

Based on a cartographic refinement of previous work, petrographic analysis, and zircon U-Pb dating of eight samples from the area, as well as on the recognition of the metamorphic character of these rocks, the following informal lithological units mappable at the 1:50,000 scale are recognized (Figure 3).

From older to younger, we describe the 1) La Jojoba metasandstone and 2) La Cebolla granite, both of Jurassic age; 3) a metasedimentary succession with interbedded felsitic metavolcanic rocks that is subdivided into a lower metasedimentary unit, a middle metalimestone unit, and an upper metasedimentary unit that yield maximum depositional Early Cretaceous ages; 4) Las Jarillas mylonitic granite and 5) La Yegua mylonitic granite, both of Paleogene age. The rancho Las Jarillas and rancho La Tinaja units proposed by Vázquez Salazar (2018) are herein re-assigned to the Lower Cretaceous succession, based on our new U-Pb dating. According to our geochemical data, the protolith of the metavolcanic rocks classify as rhyodacite/dacite in a diagram of immobile and incompatible elements of Winchester and Floyd (1977) (see Supplementary Table S1), and they are herein informally referred as metarhyolites.

La Jojoba metasandstone

This unit, which consists of fine-grained metasedimentary rocks, forms a small outcrop in the eastern part of the area where it is intruded by the La Cebolla granite. Based on this relationship and because of its lithological resemblance, this unit is tentatively assigned to the La Jojoba metasandstone which is a regional unit that was described by González-León et al. (2021) in the nearby sierras El Álamo Viejo and La Jojoba. In those localities, this unit consists of metasandstone with intercalations of metaconglomerate and metarhyolite-quartz porphyry for which these authors reported a maximum depositional age of ca. 163 Ma, obtained by U-Pb dating of detrital zircons of three sandstone samples.

La Cebolla granite

The La Cebolla granite is a N-S elongated stock, 6 km long and 2 km wide that crops out in the lower eastern parts of the El Potrero range where it is cut by the La Yegua mylonitic granite (Figure 3). It is a leucocratic, medium-grained to porphyritic, mylonitized granite composed of K-feldspar, plagioclase, quartz, biotite, muscovite, and garnet, with common xenoliths of metasedimentary rocks (Vázquez Salazar, 2018). The La Cebolla granite is intruded by mylonitized dikes and sills of feldspar-porphyry granite and biotite granodiorite. The La Cebolla granite was dated by Vázquez Salazar (2018) (zircon U-

Pb) with a weighted mean crystallization age of 155.1 ± 3.4 Ma (MSWD = 4), which was recalculated to a concordia age of 158.1 ± 1 Ma (MSWD = 2.8) in González-León et al. (2021) (age shown on Figure 3).

Lower metasedimentary unit

This unit consists of interbedded metasandstone and metapelite (Figure 4A). To a lesser extent, it includes very fine-grained to aphanitic metarhyolte and lenticular beds of pebble metaconglomerate found at the base of the metasandstone. In the southern part of the study area, this unit dips W-SW with maximum values of 45° and has an estimated thickness of 300 m. In other outcrops in the area, the metarhyolite interbeds are more abundant and occur in packages up to 30 m thick. A finer grain size, lighter color, and locally developed eutaxitic texture with flattened vitric fragments and contorted flow banding (Figure 4B) distinguishes the metavolcanic rocks from the metasandstones. The base of this unit is covered by recent alluvial sediments, and in the south part of the studied area it is intruded by the La Yegua mylonitic granite.

Metalimestone unit

This unit comprises stratified and recrystallized limestone beds (Figures 4C) that alternate with metapelites and metasandstones, and is intruded by the Las Jarillas and La Yegua mylonitic granites. This unit is well exposed in the southern part of the area in a NNW-SSE belt that dips to the SW, and on the cerro El Picacho peak, in the east-central part of the area, where the beds dip to the NW (Figures 3 and 4D). This unit that separates the lower and upper metasedimentary units in concordant relationship has an estimated thickness of 400 m in outcrops of the southern part of the area.

Upper metasedimentary unit

This unit comprises an interbedded succession of metasandstone, metapelite and metarhyolite rocks that is very similar to the lower metasedimentary unit. In the southern part of the study area, this unit has an estimated maximum thickness of 500 m. In the northern part of the study area, in La Jojoba hill, this unit dips to the SE with values less than 40° and is composed of metasandstones, metarhyolites and metapelites that reach an incomplete estimated thickness of 600 m.

Las Jarillas mylonitic granite

This granite occurs as a pluton of small dimensions with associated cm to m-thick pegmatitic and aplitic dikes and sills that crop out in the western part of the study area where it intrudes the metasedimentary units (Figure 3). It is a fine-grained and saccaroid leucocratic granite composed of feldspar, quartz, muscovite, garnet, scarce biotite, and rarely hornblende. For Las Jarillas mylonitic granite, Vázquez Salazar (2018) reported a zircon $^{206}Pb/^{238}U$ weighted mean age of 59.3 ± 1.5 Ma interpreted as its igneous crystallization age.

La Yegua mylonitic granite

The La Yegua mylonitic granite is mainly restricted to the eastern part of the studied area, where it forms N-S discontinuous and elongated outcrops, and also forms dikes and sills that intrude La Cebolla granite and the mestasedimentary rocks. It contains abundant metasedimentary xenoliths. It is a leucocratic, medium to coarse grained granite, with pegmatitic zones, K-feldspar crystals up to 5 cm, muscovite, garnet and sparse biotite.

Petrographic analysis

The metapelitic rocks vary from metapelite with abundant micaceous matrix to semipelite that are rich in dynamically recrystallized quartz and feldspar. The former is more abundant and dominated by an association of muscovite and biotite in variable proportions, with less abundant quartz and feldspar. Micas occur as elongated crystals up to 2 mm in length arranged in thin, discontinuous to continuous bands (Figure 5A). In metapelites that are rich in quartz and feldspar, these minerals commonly are oriented in bands that alternate with thinner, discontinuous bands of muscovite and/or biotite, and/or with bands of finely recrystallized quartz. Other subordinate minerals in the metapelites include epidote, that is abundant in some samples, opaque minerals interpreted as iron oxides, apatite, tourmaline, staurolite, actinolite, titanite, and garnet (Figure 5A). Muscovite may occur as mica fish (Figure 5A) and generally it is more abundant than biotite which may show partial alteration to chlorite. Some garnet porphyroblasts are up to 2 mm in diameter, commonly as poikiloblasts with quartz inclusions, rarely have helictic cleavage, and are rotated to form sigma and delta structures with muscovite pressure shadows. The cleavage developed in these rocks ranges from continuous to coarsely spaced and anastomosed. In a few thin sections it was observed quartz deformed by subgrain rotation, S-C cleavage, and incipient crenulation (Passchier and Trouw, 2005).

The metasandstone is mostly composed of fine- to coarse-grained quartz and feldspar in variable proportions that commonly arrange in discontinuous sub-parallel bands separated by thinner muscovite and/or biotite bands (Figure 5B). The quartz is elongated and forms thin, dynamically recrystallized ribbons with subgrain rotation, while the feldspar porphyroclasts show serrated edges surrounded by fine feldspar and quartz grains. Other less common minerals include epidote, opaque minerals, tourmaline, apatite, and staurolite. These rocks generally exhibit a coarse to anastomosing continuous cleavage defined by bands of quartz and mica. In some samples, spaced cleavage and occasionally S-C cleavage also occur. Muscovite can form mica fish crystals that indicate a top-to-the SW shear direction.

The metarhyolites are very fine-grained rocks that vary from samples with abundant micaceous matrix to others rich in recrystallized quartz with variable proportions of feldspars, biotite, muscovite, epidote and opaque minerals. Other minerals present in subordinate amounts include titanite, tourmaline, hornblende, zoisite, zircon, and apatite. These rocks display either a continuous cleavage, or a coarse, anastomosed spacing cleavage that is defined by the alignment of sub-parallel and discontinuous bands of recrystallized quartz that alternate with bands of oriented biotite, muscovite, and opaque minerals (Figure 5C). In some samples, the recrystallized quartz forms lenticular ribbons deformed by subgrain-rotation. In a few samples, rotated feldspars porphyroclasts with little fracturing and serrated edges are present. In samples where the matrix is abundant, it is formed by fine, elongated and oriented crystals of biotite and muscovite, where the biotite is partially altered to chlorite. Some muscovite crystals reach larger sizes and develop mica-fish tails. The σ-type crystals, mica-fish muscovite crystals, and S-C shear band cleavage indicate a general top-to-the SW shear direction.

Petrographically, samples of the metalimestone unit are mainly composed of calcite with few muscovite, quartz, and opaque crystals (Figure 5D). The grains have an inequigranular texture, with subhedral crystals up to 0.4 mm long. The calcite is colorless, with polysynthetic twins, which are locally microfolded (kink-like folds). The muscovite crystals are neither deformed nor preferentially oriented. Quartz occurs as patches surrounded by calcite and opaque minerals. These rocks can be classified as marble.

According to the classification of Fettes and Desmons (2011), the metapelite, meta-sandstone and metarhyolite rocks of the study area classify as quartz-feldspathic muscovite ± biotite < epidote schists, although proportions of these minerals are highly variable among the samples studied. Other sparse metamorphic minerals include tourmaline, staurolite, garnet, hornblende, actinolite, apatite, and zoisite.

Based on the above mineral paragenesis, the metamorphic grade shown by these rocks is interpreted to be of upper greenschist facies grading into lower amphibolite facies. Local chlorite replacement of biotite is likely caused by retrograde effects during uplift of the footwall along a normal-slip detachment fault.

Samples of Las Jarillas and La Yegua mylonitic granites are petrographically very similar. Both granites are composed of quartz, K-feldspars (microcline and orthoclase) and to a lesser extent plagioclase, muscovite, biotite and garnet (Figures 5E and 5F). The quartz is dynamically recrystallized and occurs as ribbons of fine-grained crystal aggregates surrounding up to 4 mm long feldspar porphyroclasts. The quartz bands are separated by thinner bands of very fine-grained mica and feldspar that define the foliation. Feldspar porphyroclasts have undulatory extinction and show dynamic recrystallization expressed by serrated edges surrounded by feldspar and/or quartz microcrystals, rotation and fracturing. They also occur in σ- and φ-type objects (Passchier and Trouw, 2005) with pressure shadows formed by quartz, feldspar, or micas. Some crystals show perthitic texture. Plagioclase crystals have albite and Carlsbad-albite twinning; some have domino and mosaic fracturing. Some crystals have wedge-shaped deformation twins, partially obliterated twins, microfracturing and kink-like folds. Muscovite crystals form mica-fish morphology, kink-like folds and boudins, while biotite is less abundant and partially altered to chlorite. Garnet crystals have subhedral and euhedral shapes and some of them have inclusions of quartz. The most common recrystallization mechanism of quartz is subgrain rotation, and less common bulging recrystallization and grain-boundary migration (Stipp et al., 2002). These dynamically recrystallized quartz aggregates form a serial-interlobate and/or serial-ameboid fabric. In these rocks, the quartz underwent strong ductile recrystallization whereas feldspar was deformed by ductile-brittle mechanisms. Brittle deformation is manifested by intragranular microfracturing, extension or compression fractures and domino and mosaic fragmentation in the porphyroclasts.

The granites show microstructural characteristics of mylonite and, to a lesser extent, protomylonites based on their percentage of matrix as compared to porphyroclasts (Passchier and Trouw, 2005). Kinematic indicators that consistently record a top-to-the SW shear direction (left shear direction) are porphyroclasts with dynamically recrystallising σ-type mantles (Passchier and Trouw, 2005), muscovite with mica-fish morphology, and S-C fabrics.

Geochronology

We performed U-Pb zircon geochronology of one metasandstone sample, three samples of metarhyolitic rocks and four samples of the mylonitic granites. The $^{206}Pb/^{238}U$ (2-sigma) ages obtained are summarized in Table 1 along with coordinate location of the samples. Two other samples were analyzed by $^{40}Ar/^{39}Ar$ thermochronology and the results are presented in Figures 8 and 9. The analytic data for these analyses are compiled in Supplementary Tables S2 and S3.

U-Pb geochronology

For metasandstone sample 10-10-17-4 that was collected from the lower metasedimentary unit, in the southern part of the area (Figure 3), we dated 100 zircon grains. Seven were discarded because of high discordance. Five yielded Precambrian ages, one Paleozoic, ten yielded Jurassic ages, and seventy-six yielded Early Cretaceous ages between ca. 144 and 114 Ma. Considering the Cretaceous dates, a mean $^{206}Pb/^{238}U$ age of 119.3 ± 0.4 Ma (MSWD =2.5, n= 68) is obtained for this sample, which is considered a reliable maximum depositional age for the lower metasedimentary unit (Figure 6A).

From the lower metasedimentary unit, we also dated the metarhyolite samples 3-21-18-1 and 3-22-18-1 (Figure 3). Sample 3-21-18-1 yielded significant inherited populations. 51 grains of Precambrian ages, between ca. 2550 and 590 Ma are documented; four others gave scattered Paleozoic ages, six are Triassic, and 17 gave scattered Jurassic ages. Of thirteen Early Cretaceous dates, the youngest population is interpreted to represent the volcanic source. The maximum depositional age of this sample is calculated at 118.5 ± 0.9 Ma (MSWD= 2) from the seven youngest concordant and overlapping zircon ages (Figure 6B). Similarly, 92 zircons were dated from the metarhyolite sample 3-22-18-1 collected from the lower metasedimentay unit (Figure 3), of which 24 yielded Proterozoic ages (between 2281 and 898 Ma), one zircon is Paleozoic, two others are Triassic, 38 scattered Jurassic ages, whereas 26 yielded Early Cretaceous ages between 144 and 110 Ma. One discordant zircon of ca. 96 Ma is not considered. The mean age obtained from the youngest 5 zircon grains is 112.1 ± 2.1 Ma (MSWD= 2.5) (Figure 6C), considered as the maximum depositional age for this sample.

Sample 8-4-18-1 corresponds to a metharyolitic rock collected from the upper metasedimentary unit (Figure 3). A total of 34 zircons were dated from this sample, of which five gave Proterozoic ages, 17 gave scattered Jurassic ages, ten gave Early Cretaceous ages between ca. 141 and 113 Ma, and two others, slightly discordant, with ages close to 99 Ma. The preferred age calculated on the Aptian zircon group

yielded a mean age of 118.2 ± 0.9 Ma (MSWD= 2.7), interpreted as the best approximation for a maximum depositional age of this unit (Fig. 6D).

A Kernel density estimator plot (Vermeesch, 2012) (Figure 7) of the zircon grains (N= 312) dated from the metasedimentary and metarhyolitic samples yield an important Early Cretaceous group (n= 131; 42% of the total grains) with peak age of 117 Ma, a Jurassic group (n= 81; 26%) with peak ages of 145 Ma and 165 Ma, scarce Triassic and Paleozoic grains (n= 14), and Precambrian grains of dispersed ages (n= 85; 27%). Similar groups and peak ages (117 Ma, 145 Ma, and 160 Ma) are obtained if only the dated grains from the three metavolcanic rocks are considered.

Four samples of the mylonitic granites were also dated. From sample 12-10-17-1 of the Las Jarillas mylonitic granite (Figure 3), we dated 34 zircon grains, of which 30 have ages from ca. 67 to 48 Ma, two grains are ca. 122 Ma, one is of 245 Ma and one other has an age of 1276 Ma. Without considering the grains that do not fall on concordia, the remainders define a poorly constrained but concordant group of 17 analyses that yield a mean $^{206}Pb/^{238}U$ age of 60.1±0.9 Ma (MSWD= 7), which is interpreted to be the granite crystallization age (Figure 6E). Other, slightly discordant, younger grains may indicate a variable amount of Pb loss.

Three La Yegua mylonitic granite were analyzed (samples 12-11-17-2, 7-8-18-1 and 7-8-18-2, Figure 3). Most of the analyzed zircon grains are either discordant or inherited. Only 15 analyses out of the three dated samples are concordant, within analytical error, straddling the concordia curve from ca. 47 to 52 Ma. The youngest group of seven analyses yields a mean $^{206}Pb/^{238}U$ age of 46.9±0.3 Ma (MSWD= 0.8) (Figure 6F), which is tentatively interpreted as the best approximation for the crystallization age of the La Yegua pluton. The sample data of the La Yegua granite are also discussed by Chapman et al. (this volume).

$^{40}Ar/^{39}Ar$ geochronology

To estimate the age of deformation and metamorphism, samples 4-29-19-1 and 3-19-19-2 were dated by the $^{40}Ar/^{39}Ar$ method (Figures 8 and 9: Table 1). Sample 4-29-19-1 corresponds to a fine-grained metasandstone from the lower metasedimentary unit collected from the study area's central part (Figure 3). Sample 3-19-19-2 corresponds to a mica schist that was collected approximately 20 km northeast of the study area (Figure 2) from the Jurassic Sierra Guacomea rhyolite unit dated at ca. 171 Ma (U-Pb, zircon) (Sánchez Navarro, 2018; González-León et al., 2021).

For sample 4-29-19-1 a mineral concentrate composed mainly of muscovite and quartz was obtained. In the mineral concentrate, smaller amounts of feldspar and traces of biotite were identified by X-ray diffraction (Supplementary Table S2). Two multigrain incremental heating experiments were conducted, which yielded similar degassing patterns with eight or ten heating steps defining a plateau (Figure 8). The plateau and inverse isochron ages calculated for these experiments agree within error (Supplementary Table S2). By combining the experiments, the calculated plateau (24.20 ± 0.32 Ma; 95% conf.) and correlation ages (24.14 ± 0.57 Ma; 95% conf.) are also indistinguishable within error and represent the best approximation for the timing of metamorphism and deformation.

Sample 3-19-19-2, which was collected from the Jurassic Sierra Guacomea rhyolite unit (Figure 2), out of the study area, was dated to obtain a comparative age of the regional metamorphism. Forty-one total fusion analyses were obtained for muscovite single crystals, of which only 29 had acceptable argon gas levels. A weighted mean age of 30.60 ± 0.82 Ma (95% conf.; MSWD=1.4) was calculated with a group of 28 coherent single age data (Figure 9). The same steps define an inverse isochron age of 29.3 ± 1.9 Ma (95% conf.; MSWD=1.2) that overlap within error, with a non-atmospheric initial $^{40}Ar/^{36}Ar$ value of 396 ± 56 (Figure 9).

Structural data

The rocks in the study area are affected by foliation and mylonitic lineation, with S tectonites being the most common, followed by L-S tectonites (Passchier and Trouw, 2005). Apart from these structures, the metasedimentary units also exhibit local folding. Folding of granitic and pegmatitic dikes that cut both the metasedimentary rocks and the granites was also observed.

To characterize the deformation style, 363 foliation planes and 242 lineations were measured in the different geological units of the study area (Figures 3 and 10). The foliation has a predominant NNW-SSE strike, and moderately to shallowly NE and SW dipping (Figure 10A). On the other hand, quartz and feldspars stretching lineation is mainly developed in granite, while in the metasediments it was only documented in some metarhyolite layers and in conglomerate stretched clasts. The mean lineation trend is N65E-S65W with gentle plunges to the NE and SW (Figure 10B).

General NW-SE trending antiformal and synformal structures are interpreted on a map scale from reversals in dip direction (Figure 3). The most common folding, however, is observed on a meter to decimeter scale and is most noticeable in outcrops in the southern part of the study area. According to the

symmetry and inclination of the axial plane, they are classified as asymmetric folds with overturned to recumbent axial planes. According to the inter-limb angle, most are classified as isoclinal folds, tight folds, or closed folds (Figure 11A-D). The folding is more pronounced in some metalimestone layers, where sheath folds were also observed (Figure 11E). Field data obtained show that the axial planes have variable orientations, although those with SW and NE inclinations predominate (Figure 10C). In one location, southeast of El Sauz, we observed a pegmatitic foliated dike of probably La Yegua granite sharply intruding an asymmetric, southwest-verging fold in the metasedimentary unit (Figure 12A).

Other structures in the area are the El Picacho detachment fault and NNE and NW high-angle normal faults, the most important of which is the El Sauz fault. El Picacho fault is a secondary, gently west-dipping detachment microbreccia zone that separates the metasedimentary units from the underlying La Cebolla granite near Cerro El Picacho (Figure 3). Deformation appears to be localized along a mylonitized Tertiary granite sill, probably part of the La Yegua granite, that intrudes the top of the Jurassic section. An uncertain amount of normal displacement is inferred on this structure. The El Sauz fault is a high angle normal fault that offsets the upper from the lower metasedimentary units and has a ca. 5 m wide breccia and cataclastic zone in outcrops near Rancho El Sauz, southwestern part of the study area (Figures 3 and 11F).

DISCUSSION

The area of the sierras Las Jarillas-El Potrero is part of the NNW-SSE metamorphic core complex belt in Sonora that extends from the Sierra Mazatán in the south, to the Pozo Verde complex at the Sonora-Arizona border. As in southern Arizona, the Sonoran MCCs have a NE-SW extension direction and predominantly SW transport direction (Nourse et al., 1994; Calmus et al., 2011; Spencer et al., 2019) (Figure 1), except for the small Sierra Aconchi metamorphic core complex that has a NE-transport direction (Calmus et al., 1996; Lugo Zazueta, 2006; Wong et al., 2010; Almada-Gutiérrez, 2020). The southern Arizona MCCs record extension duration between ca.33 and 18 Ma, while those of Sonora are reported as slightly younger, between 25 and 15 Ma (Wong and Gans, 2008; Wong et al., 2010).

The lower plates of the central Sonora MCCs mainly consist of Late Cretaceous to Eocene plutonic rocks and, to a lesser extent, orthogneisses and metasedimentary rocks that range in age from Precambrian to Mesozoic (Anderson et al., 1980; Vega Granillo and Calmus, 2003; Lugo Zazueta, 2006; González-Becuar et al., 2017; Almada Gutiérrez, 2020). The lower plate of the MCC belt of the Magdalena-

Tubutama region, in northern Sonora, is predominantly composed of volcanic, volcano sedimentary, and plutonic rocks of the Jurassic magmatic arc, Cretaceous metasedimentary rocks, and Cenozoic granitic plutons that are generally leucocratic and two-mica bearing with low-dipping foliations and N30°-50°E lineations (Nourse, 1989; Anderson et al., 2005; Herrera Urbina et al., 2006; Nourse et al., 2018; Sánchez Navarro, 2018; Vázquez Salazar, 2018; Zapata Martínez et al., 2018; Jacobson et al., 2019; González-León et al., 2021).

Nourse (1995) included the study area as part of the lower plate of the MCCs of the Magdalena-Tubutama region (Figure 2) and inferred that the trace of the regional detachment fault that formed these complexes crosses just south of the Sierras Las Jarillas-El Potrero with a displacement direction toward the southwest. This interpretation is consistent with the ubiquitous top-to-the-southwest shear indicators obtained in the study area. Although the primary Magdalena-Tubutama detachment is concealed by alluvium, we have mapped the secondary El Picacho detachment fault (Figure 3). Secondary, shallow-dipping detachment faults such as this have been recognized in the lower plates of other metamorphic core complexes. A good example is the brittle fault that separates the Cocospera Conglomerate from underlying Jurassic rhyolite in the northeast part of the Magdalena-Madera core complex (Nourse, 1989; 1990).

The most widely distributed rocks in the study area correspond to those informally referred to as the lower metasedimentary unit, the metalimestone unit, and the upper metasedimentary unit. The lower and upper units are composed of similar successions of metapelites, metasandstone and metavolcanic rocks separated by the intermediate metalimestone unit. Based on the similar lithological succession and because of the Aptian maximum depositional age obtained from the metasandstone sample 10-10-17-4, Vázquez Salazar (2018) suggested a correlation of these units with the Aptian-Albian Morita, Mural Limestone and Cintura formations of the Bisbee Group (Jacques-Ayala, 1995; Lawton et al., 2004; Mauel et al., 2011). Maximum depositional ages reported for the base and top of the Morita Formation in northern Sonora are of ca. 125 Ma and 115 Ma, respectively, and of ca. 109 Ma for the basal Cintura Formation (Peryam et al., 2012; González-León et al., 2020; González-León et al., 2023). .

The important Early Cretaceous U-Pb age group that indicates a main peak age of 117 Ma for our dated samples from the metasedimentary succession (Figure 7), and the mean ages of the individual samples that range from ca. 119 Ma to 112 Ma leads support to the suggested correlation of these rocks with the Bisbee Group formations. Similar detrital zircon age peaks between 120 Ma and 111 Ma as well

as Jurassic and Precambrian age groups like the herein obtained (Figure 7), are present in sandstone and ash fall tuffs from the Bisbee Group in other parts of Sonora (see for instance Peryam et al, 2012; González-León et al., 2023).

The closest unmetamorphosed outcrops of the Bisbee Group are at Cerro Pimas and Cerro El Ocuca, located 10 km south and 20 km southwest of the study area. At these localities, the Morita and Cintura formations are composed of similar successions of sandstone, siltstone, ash fall tuffs and subordinate conglomerate of fluvial origin (Jacques-Ayala, 1995), while the Mural Limestone is composed of 420 to 640 m thick sections of fossiliferous limestone beds with interbedded shale (González-León et al., 2008; Madhavaraju et al., 2013). Although the metasedimentary units of the study area are deformed, their protoliths and succession are very similar to the Lower Cretaceous Bisbee Group formations. The metavolcanic beds in the study area may correspond to dynamically recrystallized ash fall tuffs that are commonly interbedded in the Bisbee Group formations in other areas of Sonora (see Peryam et al., 2012; González-León et al., 2020). Abundant inheritance of older zircon grains, like the observed in the metavolcanic rocks herein reported is also present in an ash fall tuff of the upper Morita Formation of north-central Sonora (Peryam et al., 2012).

The two-mica and garnet Las Jarillas and La Yegua mylonitic granites, with ages of ca. 60 and ca. 47 Ma, correspond to the late Laramide arc magmatism of Sonora. Zapata Martínez et al. (2018) and Nourse et al. (2018) reported that the plutons that intrude the MCCs of the Magdalena-Tubutama region are two-mica-garnet leucocratic granites, and sparse granodioritic plutons with ages between ~59 and ~38 Ma. Based on the geochemical composition of some of these granites, including the Las Jarillas and La Yegua granites, Sánchez Navarro (2018) and Vázquez Salazar (2018) interpreted them as anatectic granites that were emplaced in a mature continental arc. Similarly, Nourse et al. (2018) considered these granites as produced by crustal anatexis preceding the mylonitic deformation and exhumation of the Magdalena-Madera MCC. Barth et al. (2018) also reported ages between 59 and 51 Ma for three two-mica leucocratic granites in the Sierra San Juan, located ~20 km northwest of the town of Tubutama (Figure 2). They suggested that the Paleogene-Eocene peraluminous magmatism of northern Sonora and southern Arizona was associated with crustal thickening during the Laramide orogenic event. More recently, Chapman et al. (2021) included the peraluminous granites of this region, of northern Sonora, within the North America Cordilleran Anatectic Belt. The mylonitic granites in the area have abundant inherited zircons, which is also a characteristic of these anatectic granites (Chapman et al., 2021). Besides zircon inheritance, Chapman et al. (2023) also noted that anatectic granites, like the ca. 58 Ma Pan Tak

granite of the Coyote Mountains in nearby southern Arizona record a protracted history of prograde metamorphism, melting and melt crystallization which makes difficult to obtain undisputed crystallization ages for these plutons.

Folds within the study area record post-Eocene deformation related to the MCC extensional event, but an earlier phase of Laramide (Late Cretaceous-early Tertiary) deformation should be considered given the location within a regional Laramide fold-thrust belt (Jacques-Ayala and Potter, 1987; Jacques-Ayala, 1995; Nourse, 2001; Iriondo et al., 2005; Mauel et al., 2011; Peryam et al., 2012; Jacobson et al., 2019; Lawton et al., 2020). For example, pre-47 Ma deformation is suggested by a southwest-verging overturned fold observed in metasedimentary strata southeast of El Sauz that is sharply intruded by a dike of probably La Yegua granite (Figure 12A). However, the dike itself exhibits a moderate foliation, indicating superimposed deformation. Several other open, hectometer-scale folds with NNW axes may be related to footwall deformation during extensional exhumation. This interpretation is supported by consistent southwest-vergent S-C structures observed on NE and SW-dipping limbs of these folds. At outcrop scale, isoclinal to tight folds with overturned to recumbent geometries and axial planes of varying directions and inclinations may indicate more than one event. In other places, veins and dikes of La Yegua granite exhibit asymmetric buckling and boudinage (Figure 12B) similar to features in the lower plate of the Magdalena core complex in the Sierra Magdalena, that are attributed to Tertiary shearing (Nourse, 1990). Some folds observed in Sierras Las Jarillas-El Potrero may also represent Laramide structures later rotated and transposed into the dominant Tertiary mylonitic fabric. Overall, the S-C fabrics and folds observed in the rocks of the study area are interpreted as the product of exhumation of the lower plate of the metamorphic core complex and produced by the Magdalena-Tubutama detachment fault proposed by Nourse (1995). Our kinematic analysis of the microstructures and the vergence of the axial planes of the folds suggest a southwestward transport direction, which agrees with the kinematics of the Magdalena-Tubutama fault (Figure 3, section A-A'). In this work, however, neither a cataclastic breccia zone nor rocks that represent an upper plate and that could indicate the location or presence of the main detachment zone were identified.

The quartz dynamic recrystallization in the studied samples gives an indication of the temperature conditions at which deformation and metamorphism may have occurred. According to Passchier and Trouw (2005), the temperature of a shear zone may be inferred by the quartz mechanical deformation. However, other factors are involved in the process, such as pressure and the presence of water. Quartz grains in most of the studied samples show subgrain rotation deformation and, to a lesser extent, bulging

and grain boundary migration, while feldspars show ductile-fragile deformation. This type of deformation suggests that the rocks in the area were deformed at temperatures between 280 and 500°C and depths between 10 and 15 km (Passchier and Trouw, 2005; Stipp et al., 2002; Fossen and Cavalcante, 2017).

The $^{40}Ar/^{39}Ar$ cooling age of 24.14 ± 0.57 Ma, obtained for muscovite+quartz from a metasandstone from the lower metasedimentary unit, indicates that extension and deformation was in progress in the study area by late Oligocene time. This age lies within the ca. 25-23 Ma age range of extension and rapid cooling obtained by Wong et al. (2010) on K-feldspar and muscovite for the Magdalena-Madera MCC lower plate. The obtained cooling age supports the idea of the metamorphic rocks of the Sierras Las Jarillas-El Potrero being contemporaneous to and part of the Magdalena-Madera MCC, from which they were separated by normal faulting associated with late-stage Basin and Range extension.

The $^{40}Ar/^{39}Ar$ weighted mean age of 30.6 ± 0.82 Ma and the nearly similar intercept age of 29.3 ± 1.9 Ma obtained on muscovite from a sample collected of a mica schist of the Late Jurassic Sierra Guacomea rhyolite unit (Sánchez Navarro, 2018; González-León et al., 2021), north of the study area, provide additional information on the age of regional metamorphism. This age is notably older than those obtained for the Magdalena-Madera MCC; therefore, it likely records an older age of exhumation and cooling for the northern part of this complex. Muscovite $^{40}Ar/^{39}Ar$ cooling ages between ca. 31 and 29 Ma have been also reported for mylonite samples of the Coyote Mountains MCC in southern Arizona by Gotardi et al. (2020).

CONCLUSIONS

The rocks of the sierras Las Jarillas-El Potrero of north-central Sonora consist of metamorphosed rocks whose protoliths range in age from Jurassic to Eocene. The oldest is the Late Jurassic La Jojoba metasandstone that is intruded by the 158.1 ± 1 Ma (U-Pb) La Cebolla granite (González-León et al., 2021). A younger metasedimentary succession with subordinate metavolcanic rocks yielded U-Pb (zircon) maximum depositional ages of Early Cretaceous and is divided into three informal units that probably correlate with the Bisbee Group formations because of comparable stratigraphic succession and geochronological age.

The Cretaceous units are muscovite ± biotite ± epidote quartzo-feldspathic schists that exhibit continuous and/or spaced cleavage mainly defined by preferential bands of mica alignment. The mineral assemblage of muscovite, biotite, and epidote with the rare occurrence of tourmaline, garnet, staurolite, titanite, hornblende, actinolite, apatite, and zoisite suggests that rocks of the area underwent upper greenschist facies metamorphism, grading into lower amphibolite facies. Kinematic indicators, like mica-fish and S-C cleavage indicate a consistent top-to-the-SW sense of shear.

The Paleogene two-mica + garnet Las Jarillas and La Yegua mylonitic granites that intrude the older rock units have U-Pb crystallization ages of 60.1 ± 0.9 and 46.9 ± 0.3 Ma, respectively. Foliation in these L-S tectonites is mainly defined by dynamically recrystallized quartz bands that surround feldspar porphyroclasts. Quartz predominantly recrystallized by subgrain rotation and rarely by bulging and grain-boundary migration, while the feldspars show ductile-fragile deformation. Mica-fish muscovite crystals and σ-type porphyroclasts are common in the granite and indicate a top-to-the-SW shear direction of tectonic transport.

Foliation in the area strikes predominantly NNW-SSE, with average dips of 28° to the NE and SW. The lineation is consistently ENE-WSW with average inclinations of 16° to the NE and SW. The most common folding in the area are asymmetric, tens of centimeters to meter scale folds with overturned to recumbent axial planes whose inclinations indicate predominantly SSE-SSW vergence.

The sierras Las Jarillas-El Potrero area was considered by Nourse (1995) as part of the lower plate of several domains of metamorphic core complexes associated with the Magdalena-Tubutama detachment fault that borders the southern part of the study area with a slip direction to the SW. The mylonitic deformation, vergence of tectonic structures, and kinematic slip direction in rocks of the Sierras Las Jarillas-El Potrero are consistent with the main detachment fault located south of the area (Nourse, 1995) while a secondary fault within the area is the El Picacho detachment fault. A younger structural event that affects the rocks of the area corresponds to NE- to NW-trending high-angle normal faulting, representative of which is the El Sauz fault. This event may be related to the uplift of the Sierras Las Jarillas-El Potrero during late Basin and Range extension.

The $^{40}Ar/^{39}Ar$ age of 24.14 ± 0.57 Ma obtained from a muscovite+quartz mixture separated from a metasandstone of the lower metasedimentary unit indicates that extension and exhumation was ongoing in the sierras Las Jarillas-El Potrero area at that time. This age is contemporaneous with $^{40}Ar/^{39}Ar$ (K-feldspar and muscovite) cooling ages reported by Wong et al. (2010) from the Magdalena-Madera MCC,

located ~15 km east of the study area, that indicate that rapid extension occurred between 25 and 23 Ma. Contemporaneity of these ages support the idea that both areas may be part of the same metamorphic core complex. The $^{40}Ar/^{39}Ar$ age of 29.3 ± 1.9 Ma in muscovite, obtained from a Jurassic-aged micaschist located ~20 km northeast of the study area is older than the ca. 24 Ma age obtained for the study area and could indicate that exhumation in that region started during the early Oligocene, earlier than previously considered and comparable to the Coyote Mountains metamorphic core complex of southern Arizona (Gottardi et al., 2020).

ACKNOWLEDGMENTS

Results of this contribution were obtained through financial support of CONACYT (presently Secretaría de Ciencia, Humanidades, Tecnología e Inovación, Gobierno de México) Project No. 253545. T. Sánchez Navarro also acknowledges and thanks support from CONACYT scholarship No. CVU 929191. We appreciate preliminary reviews of this paper by Drs. Thierry Calmus, José Luis Rodríguez Castañeda (R.I.P.), Ricardo Vega Granillo and Uwe Martens. We also thank and acknowledge valuable support from Aimé Orci Romero and Elizard González Becuar of ERNO who provided sample thin sectioning, sample powdering and mineral separation; to Dr. Mélanie Noury and Dr. José Luis Rodríguez Castañeda for their instructive help during a field-trip accompaniment to the study area, and to Dr. Jesús Vidal Solano for his valuable comments on the geochemical data. We also acknowledge sample preparation and characterization for $^{40}Ar/^{39}Ar$ dating by Susana Rosas Montoya and Gabriel Rendón (CICESE), and Marina Vega González (Instituto de Geociencias, UNAM), as well as argon isotope measurement by Gabriela Hernández Quevedo (Instituto de Geociencias, UNAM) and Miguel Ángel García (CICESE). The argon geochronology lab LIGAr was supported by CONACYT infrastructure grants 224667 and 316372. Reconnaissance field work by Jon Nourse in 1986 was supported by the California Institute of Technology. Ann Egger's field season in the study area during January and February of 2001 was funded by Stanford University. Valuable help and permit to do fieldwork in their ranches was received from Sr. Alonso Portillo and ejidatarios of El Coyotillo, Héctor "Tito" Gerlach, Arturo Gerlach, Enrique "Jorique" Noriega, and Javier "El Carrillero" Cruz and it is greatly appreciated. This contribution benefited greatly for insightful reviews by Dr. Carl Jacobson and an anonymous

reviewer whose critical observations we deeply appreciate. Editorial handling and valuable comments by Dr. Thierry Calmus are also greatly appreciated.

REFERENCES

Allmendinger, R. W. (2019). *Stereonet 10, Program for stereographic projection*. Cornell University Ithaca, N.Y.

Almada Gutiérrez, V. S. (2020). *Geología y termocronología a lo largo de un transecto en el centro de la sierra de Aconchi, Sonora, México* [M. Sc. Thesis] Universidad Nacional Autónoma de México, Posgrado en Ciencias de la Tierra.

Anderson, T. H., & Silver, L. T. (1979). The role of the Mojave-Sonora megashear in the tectonic evolution of northern Sonora. In T. H., Anderson, & J., Roldán-Quintana, (eds.), *Geology of Northern Sonora, Guidebook-Field Trip 27* (59–68). Geological Society of America.

Anderson, T. H., Silver, L. T., & Salas, G. A., (1980). Distribution and U-Pb isotope ages of some lineated plutons, northwestern Mexico. *Geological Society of America Memoir*, *153*, 269–283.

Anderson, T. H., & Silver, L. T. (2005). The Mojave-Sonora megashear-Field and analytical studies leading to the conception and evolution of the hypothesis. In T. H., Anderson, J. A., Nourse, J. W., McKee, & M. B. Steiner, (eds.), The Mojave-Sonora megashear hypothesis: Development, assessment, and alternatives. *Geological Society of America Special Paper, 393*, 1–50.

Arvizu, H. E., & Iriondo, A. (2015). Control temporal y geología del magmatismo Permo-Triásico en Sierra Los Tanques, NW Sonora, México: Evidencia del inicio del arco magmático cordillerano en el SW de Laurencia. *Boletín de la Sociedad Geológica Mexicana*, *67*, 545–586.

Barth, A. P., Haxel, G. B., Roldan-Quintana, J., Wooden, J. L, Jacobson, C. E., & Mallery, C. W. (2018). Insights into regional Laramide crustal melting: whole-rock and SIMS zircon geochemistry of late Laramide peraluminous granites in southern Arizona and northern Sonora. *Geological Society of America Abstracts with Programs*, *50*(5), doi: 10.1130/abs/2018RM-313678

Bryan, S. E., & Ferrari, L. (2013). Large igneous provinces and silicic large igneous provinces: Progress in our understanding over the last 25 years. *Geological Society of America Bulletin*, *125*(7-8), 1053–1078. doi: https://doi.org/10.1130/B30820.1

Busby-Spera, C. J. (1988). Speculative tectonic model for the early Mesozoic arc of the southwest Cordilleran United States. *Geology*, *16*, 1121–1125. doi: 10.1130/0091- 7613(1988)0162.3.CO;2

Calmus, T., Pérez-Segura, E., & Roldán-Quintana, J. (1996). The Pb–Zn ore deposits of San Felipe, Sonora, Mexico: "Detached" mineralization in the Basin and Range Province. *Geofísica Internacional, 35*, 115–124.

Calmus, T., Vega-Granillo, R., & Lugo-Zazueta, R. (2011). Evolución geológica de Sonora durante el Cretácico Tardío y el Cenozoico. In T. Calmus, (eds.), Panorama de la Geología de Sonora, México. *Universidad Nacional Autónoma de México, Instituto de Geología, Boletín*, *118*, 227–266.

Chapman, J. B., Greig, R., & Haxel, G. B. (2020). Geochemical evidence for an orogenic plateau in the southern U.S. and northern Mexican Cordillera during the Laramide orogeny. *Geology, 48*(2). 164–168. doi: https://doi.org/10.1130/G47117.1.

Chapman, J. B., Runyon, S. E., Shields, J. E., Lawler, B. L., Pridmore, C. J., Scoggin, S. H., Swaim, N. T., Trzinski, A. E., Wiley, H. N., Barth, A. P., & Haxel, G. B. (2021). The North American Cordilleran Anatectic Belt. *Earth-Science Reviews, 215*, 103576. https://doi.org/10.1016/j.earscirev.2021.103576.

Chapman, J. B., Pridmore, C., Chamberlain, K., Haxel, G., & Ducea, M. (2023). Himalayan-like Crustal Melting and Differentiation in the Southern North American Cordilleran Anatectic Belt during the Laramide Orogeny: Coyote Mountains, Arizona. *Journal of Petrology, 64*, 1–22. https://doi.org/10.1093/petrology/egad075

Coney, P. J., & Harms, T. K. (1984). Cordilleran metamorphic core complexes: Cenozoic extensional relics of Mesozoic compression. *Geology, 12*(9), 550–554. doi: https://doi.org/10.1130/0091-7613(1984)12<550:CMCCCE>2.0.CO;2

Damon, P. E., Shafiqullah, M., Roldán Quintana, J, & Cochemé, J. J. (1983). El batolito Laramide (90-40 Ma) de Sonora. *Asociación de Ingenieros de Minas, Metalugistas y Geólogos de México (AIMMGM), Memoria técnica 15*, 63–95.

Davis, G. A., Lister, G. S., & Reynolds, S. J. (1986). Structural evolution of the Whipple and South mountains shear zones, southwestern United States. *Geology*, *14*, 7–10. doi: https://doi.org/10.1130/0091-7613(1986)14<7:SEOTWA>2.0.CO;2

Davis, G. H. (1980). Structural characteristics of metamorphic core complexes, southern Arizona. *Geological Society of America Memoir, 153*, 35–77.

Davis, G. H. (1983). Shear-zone model for the origin of metamorphic core complex. *Geology, 11*(6), 342–347. doi: https://doi.org/10.1130/0091-7613(1983)11<342:SMFTOO>2.0.CO;2

Davis, G.H., Gardulski, A.F., & Anderson, T.H. (1981). Structural and structural-petrological characteristics of some metamorphic core complex terranes in southern Arizona and northern Sonora. In L., Ortlieb, & J. Roldan-Quintana, (Eds.), *Geology of Northwestern Mexico and Southern Arizona* (pp. 323–363). Geological Society of America, Cordilleran Section, 1981 Field Trip Guidebook.

Dickinson, W. R. (1991). Tectonic setting of faulted Tertiary strata associated with the Catalina core complex in southern Arizona. *Geological Society of America Special Paper, 264*, 106. https://doi.org/10.1130/SPE264

Dickinson, W. R., & Lawton, T. F. (2001). Carboniferous to Cretaceous assembly and fragmentation of Mexico. *Geological Society of America Bulletin*, *113*, 1142–1160. doi: https://doi.org/10.1130/0016-7606(2001)113<1142:CTCAAF>2.0.CO;2

Dickinson, W. R. (2002). The Basin and Range Province as a Composite Extensional Domain. *International Geology Review, 44*(1), 1–38. DOI: 10.2747/0020-6814.44.1.1

Ferrari, L., Orozco-Esquivel, T., Bryan, S. E., López-Martínez, M., & Silva-Fragoso, A. (2018). Cenozoic magmatism and extension in western Mexico: Linking the Sierra Madre Occidental silicic large igneous province and the Comondú Group with the Gulf of California rift. *Earth-Science Reviews, 183*, 115–152.

Fettes, D. & Desmons, J., (Eds.) (2011). *Metamorphic rocks: A classification and glossary of terms*. Cambridge University Press.

Fossen, H., & Cavalcante, G. C. G. (2017). Shear zones-A review. *Earth-Science Reviews, 171*, 434–455. https://doi.org/10.1016/j.earscirev.2017.05.002

García and Barragán, J.C., & Jacques-Ayala, C. (2011). Estratigrafía del Cretácico de Sonora, México. In T. Calmus, (Ed.), Panorama de la geología de Sonora, México. *Universidad Nacional Autónoma de México, Instituto de Geología*, 113–199.

González-Becuar, E., Pérez-Segura, E., Vega-Granillo, R., Solari, L., González-León, C. M., Solé, J. & López Martínez, M. (2017). Laramide to Miocene syn-extensional plutonism in the Puerta del Sol area, central Sonora, Mexico. *Revista Mexicana de Ciencias Geológicas*, *34*, 45–61.

González-León, C. M., Scott, R. W., Löser, H., Lawton, T. F., Robert, E., & Valencia, V. A. (2008). Upper Aptian-Lower Albian Mural Formation: stratigraphy, biostratigraphy and depositional cycles on the Sonoran shelf, northern México. *Cretaceous Research, 29*, 249–266.

González-León, C. M., Valencia, V., López, M., Bellon, H., Valencia Moreno, M.A., Calmus, T. (2010). The Arizpe sub-basin: sedimentary and magmatic evolution of the Basin and Range in north-central Sonora, México. *Revista Mexicana de Ciencias Geológicas, 27*, 292–312.

González-León, C.M., Solari, L., Valencia-Moreno, M., Rascón Heimpel, M.A., Solé, J., González Becuar, E., Lozano Santacruz, R., & Pérez Arvizu, O. (2017). Late Cretaceous to early Eocene magmatic evolution of the Laramide arc in the Nacozari quadrangle, northeastern Sonora, Mexico and its regional implications. *Ore Geology Review, 81*, 1137–1157.

González-León, C. M., Madhavaraju, J., Ramírez Montoya, E., Solari, L. A., Villanueva-Amadoz, U., Monreal, R. & Sánchez Medrano, P. A. (2020). Stratigraphy, detrital zircon geochronology and provenance of the Morita formation (Bisbee Group) in northeastern Sonora, Mexico. *Journal of South American Earth Sciences, 103*, 1–17.

González-León, C. M., Vázquez-Salazar, M., Sánchez Navarro, T., Solari, L. A., Nourse, J. A., Del Rio-Salas, R., Lozano-Santacruz, R., Pérez Arvizu, O. & Valenzuela Chacón, J. C. (2021). Geology and geochronology of the Jurassic magmatic arc in the Magdalena quadrangle, north-central Sonora, Mexico. *Journal of South American Earth Sciences, 108*, 1–18.

González-León, C.M., Sierra Rojas, M.I., Scott, R.W., Solari, L.A., Lawton, T.F., Noury, M., & Vázquez Salazar, M. (2023). Lower Cretaceous (Aptian-Albian) Bisbee Group, Arizpe area, northern Sonora, Mexico: Integrated Biostratigraphy, age and provenance from U-Pb and Hf isotopes. *Revista Mexicana de Ciencias Geológicas, 40*(3), 254– 272.

Goodwin, L. B., & Haxel, G. B. (1990). Structural evolution of the Southern Baboquirari Mountains, south-central and north-central Sonora. *Tectonics, 9*, 1077–1095.

Gottardi, R., McAleer, R., Casale, G., Borel, M., Iriondo, A., & Jepson, G. (2020). Exhumation of the Coyote Mountains metamorphic core complex (Arizona): Implications for orogenic collapse of the southern North American Cordillera. *Tectonics, 39*, 1–33.

Hayama, Y., Shibata, K., & Takeda, H. (1984). K-Ar ages of the low-grade metamorphic rocks in the altar massif, northwest Sonora, Mexico. *Journal of the Geological Society of Japan, 90*, 589–596.

Haxel, G. B., Tosdal, R. M., May, D. J., & Wright, J. E. (1984). Latest Cretaceous and early Tertiary orogenesis in southcentral Arizona: Thrust faulting, regional metamorphism, and granitic plutonism. *Geological Society of America Bulletin, 95*, 631–653.

Haxel, G.B., Anderson, T.H., Riggs, N.R., & Goodwin, L.B. (1988). The Papago terrane: A crustal anomaly in south-central Arizona and northcentral Sonora. *Geological Society of America Abstracts with Programs, 20*, 168.

Herrera Urbina, S., Valencia, V., Paz Moreno, F. A., Gehrels, G., & García Salido, R. (2006). Plutonismo hiperaluminoso asociado al "metamorphic core complex" de Magdalena, Sonora norte-central, México. *Geos, 26*, 98–99.

Instituto Nacional de Estadística y Geografía. (1975a). *Carta Topográfica Santa Ana H12A69 a escala 1: 50,000*. Secretaría de Economía, México.

Instituto Nacional de Estadística y Geografía. (1975b). *Carta Topográfica El Carrizo H12A59 a escala 1: 50,000*. Secretaría de Economía, México.

Iriondo, A., Martínez-Torres, L. M., Kunk, M. J., Atkinson, W. W., Premo, W. R., & McIntosh, W. C. (2005). Northward Laramide thrusting in the Quitovac region, northwestern Sonora, Mexico: Implications for the juxtaposition of Paleoproterozoic basement blocks and the Mojave-Sonora megashear hypothesis. In T. H., Anderson, J. A., Nourse, J. W. McKee, & M. B. Steiner (Eds.), The Mojave-Sonora megashear hypothesis: Development, assessment, and alternatives. *Geological Society of America Special Paper, 393*, 631–669.

Iriondo, A., & Premo, W. R. (2011). Las rocas cristalinas proterozoicas de Sonora y su importancia para la reconstrucción del margen continental SW de Laurencia-La pieza mexicana del rompecabezas de Rodinia. In Calmus, T. (Eds.), Panorama de la geología de Sonora, México *Universidad Nacional Autónoma de México, Instituto de Geología, Boletín, 118*, 25–55.

Jacobson, C. E., Jacques-Ayala, C., Barth, A. P., García and Barragán, J. C., Pedrick, J. N., & Wooden, J. L. (2019). Protolith age of the Altar and Carnero complexes and Late Cretaceous–Miocene deformation in the Caborca-Altar region of northwestern Sonora, Mexico. *Revista Mexicana de Ciencias Geológicas, 36*, 95–109.

Jacques-Ayala, C., & Potter, P.E. (1987). Stratigraphy and paleogeography of Lower Cretaceous rocks, Sierra El Chanate, northwest Sonora, Mexico. In W.R., Dickinson, & M.A., Klute, (Eds.), Mesozoic rocks of southern Arizona and adjacent areas*. Arizona Geological Society Digest, 18*, 203–214.

Jacques-Ayala, C. (1995). Paleogeography and provenance of the Lower Cretaceous Bisbee Group in the Caborca-Santa Ana area, northwestern Sonora. In C., Jacques-Ayala, C. M., González-León, & J. Roldán-Quintana, (Eds.), Studies on the Mesozoic of Sonora and Adjacent Areas. *Geological Society of America Special Paper, 301*, 79–98.

Jiménez García, O. G., Gradías Figueroa, J. S., & Sánchez, R. (1999). *Informe de la carta geológico-minera y geoquímica Santa Ana H12A69 escala 1:50,000*. Secretaria de Comercio y Fomento industrial, Consejo de Recursos Minerales, 1–46.

Lawton, T.F., González-León, C.M., Lucas, S.G., & Scott, R.W., 2004, Stratigraphy and sedimentology of the upper Aptian-upper Albian Mural Limestone (Bisbee Group) in northern Sonora, Mexico. *Cretaceous Research, 25*, 43–60.

Lawton, T. F., Cashman, P. H., Trexler, J. H., & Taylor, W. J. (2017). The late Paleozoic Southwestern Laurentian Borderland. *Geology, 45*, 675–678. doi: https://doi.org/10.1130/G39071.1

Lawton, T. F., Amato, J. M., Machin, S. E. K., Gilbert, J. C., & Lucas, S. G. (2020). Transition from Late Jurassic rifting to middle Cretaceous dynamic foreland, southwestern U.S. and northwestern Mexico. *Geological Society of America Bulletin, 132*, 2489–2516.

Lugo Zazueta, R. E. (2006). *Extension basin and range en la Sierra de Aconchi, Sonora, México: análisis termocronológico basado en $^{40}Ar/^{39}Ar$ y trazas de fisión* [Msc Thesis]. Universidad Nacional Autónoma de México, Posgrado en Ciencias de la Tierra.

Madhavaraju, J., Lee, Y. I., & González-León, C. M. (2013). Diagenetic significance of carbon, oxygen and strontium isotopic compositions in t he Aptian-Albian Mural Formation in Cerro Pimas, northern Sonora, Mexico. *Journal of Iberian Geology, 39*, 73-88.

Mauel, D. J., Lawton, T. F., González-León, C., Iriondo, A., & Amato, J. M. (2011). Stratigraphy and age of Upper Jurassic strata in north-central Sonora, Mexico. Southwestern Laurentian record of crustal extension and tectonic transition. *Geosphere, 7*, 390–414.

McDowell, F. W., Roldán-Quintana, J., & Amaya-Martínez, R. (1997). Interrelationship of sedimentary and volcanic deposits associated with Tertiary extension in Sonora, Mexico. *Geological Society of America Bulletin, 109*, 1349–1360.

McDowell, F. W., Roldán-Quintana, J., & Connelly, J. N. (2001). Duration of Late Cretaceous-early Tertiary magmatism in east-central Sonora, Mexico. *Geological Society of America Bulletin, 113*, 521–531.

Miranda-Gasca, M. A. & De Jong, K.A. (1992). The Magdalena mid-Tertiary extensional basin. In K. F., Clark, J., Roldán-Quintana, & R. H., Schmidt, (Eds.), *Geology and mineral resources of northern Sierra Madre Occidental, Mexico*. Guidebook for the 1992 Field Conference, The El Paso Geological Society, 377–384.

Morales-Montaño, M. (1984). Bosquejo geológico del cuadrángulo "Estación Llano-Ímuris*". Boletín del Departamento de Geología, Universidad de Sonora, 1*, 25–49.

Nourse, J. A. (1989). *Geological evolution of two crustal scale shear zones, Part II: The Magdalena metamorphic core complex* [PhD. Thesis]. California Institute of Technology.

Nourse, J.A., 1990, Tectonostratigraphic development and strain history of the Magdalena metamorphic core complex, northern Sonora, Mexico,. In G.E. Gehrels, & J.E., Spencer, (Eds.), Geologic excursions through the Sonoran Desert region, Arizona and Sonora: Arizona. *Geological Survey Special Paper, 7*, 155–164.

Nourse, J. A., Anderson, T. H., & Silver, L. T. (1994). Tertiary metamorphic core complexes in Sonora, northwestern Mexico. *Tectonics, 13*, 1161-1182.

Nourse, J. A. (1995). Jurassic-Cretaceous paleogeography of the Magdalena region, northern Sonora, and its influence on the positioning of Tertiary metamorphic core complexes. In C., Jacques-Ayala, C. M., González-León, & J., Roldán-Quintana, (Eds.), Studies on the Mesozoic of Sonora and Adjacent Areas. *Geological Society of America Special Paper, 301*, 59–78.

Nourse, J. A., González-León, C. M., Solari, L., & Zapata-Martínez, J. A. (2018). Magmatic and structural evolution of the Magdalena-Madera metamorphic core complex, Sonora, Mexico. *Geological*

Society of America Abstracts with Programs, 50(5), ISSN 0016-7592. doi: 10.1130/abs/2018RM-313985

Passchier, C. W., & Trouw, R. A. J. (2005). *Microtectonics*. Springer Berlin Heidelberg.

Peryam, T. C., Lawton, T. F., Amato, J. M., González-León, C. M., & Manuel, D. J. (2012). Lower Cretaceous strata of the Sonora Bisbee Basin: A record of the tectonomagmatic evolution of northwestern Mexico. *Geological Society of America Bulletin, 124*, 532–548.

Platt, J. P., Behr, W. M., & Cooper, F. J. (2015). Metamorphic core complexes: windows into the mechanics and rheology of the crust. *Journal of the Geological Society, 172*, 9–27. https://doi.org/10.1144/jgs2014-036.

Riggs, N. R. and Haxel, G. B. (1990). The Early to Middle Jurassic magmatic arc in southern Arizona: Plutons to sand dunes. In G.E., Gehrels, & J.E., Spencer, (Eds.), Geologic excursions through the Sonoran Desert region, Arizona and Sonora. *Arizona Geological Survey Special Paper*, *7*, 90–103.

Riggs, N. R., & Busby-Spera, C. J. (1991). Facies analysis of an ancient, dismembered, large caldera complex and implications for intra-arc subsidence: Middle Jurassic strata of Cobre Ridge, southern Arizona, USA. *Sedimentary Geology, 74*, 39–68.

Roldán-Quintana, J. (1991). Geology and chemical composition of the Jaralito and Aconchi batholiths in east-central Sonora, Mexico. In E., Pérez-Segura, & C., Jacques-Ayala (Eds.), Studies of Sonoran Geology. *Geological Society of America Special Paper, 254*, 69–80.

Salas, G. A. (1968). Areal geology and petrology of the igneous rocks, Santa Ana quadrangle, Sonora, México[M.Sc. thesis]. The University of Oklahoma.

Sánchez Navarro, T. (2018). Geología y Geocronología de las sierras El Álamo Viejo y Los Chinos, región de Tubutama, norte de Sonora [Bachelor Thesis]. Universidad de Sonora, Departamento de Geología.

Scott, R. W., González-León, C. M., Lawton, T. F., Madhavaraju, J., Saucedo-Samaniego, J. C., & Sierra Rojas, M. I. (2024) Aptian–Albian sequence stratigraphy, biostratigraphy, chemostratigraphy, and chronostratigraphy: Sonoran shelf and Tamaulipas Basin, Mexico. *Cretaceous Research, 155*, 105776. https://doi.org/10.1016/j.cretres.2023.105776

Solari, L. A., González-León, C. M., Ortega-Obregón, C., Valencia-Moreno, M., & Rascón-Heimpel, M. A. (2018). The Proterozoic of NW Mexico revisited: U–Pb geochronology and Hf isotopes of Sonoran rocks and their tectonic implications. *International Journal of Earth Sciences, 107*, 845–861.

Spencer, J. E., Richard, S. M., Lingrey, S. H., Johnson, B. J., Johnson, R. A., & Gehrels, G. E. (2019). Reconstruction of mid - Cenozoic extension in the Rincon Mountains area, southeastern Arizona, USA, and geodynamic implications. *Tectonics, 38,* 2338–2357. https://doi.org/10.1029/2019TC005565

Stewart, J. H. and Roldán-Quintana, J. (1994). Map showing late Cenozoic extensional tilt patterns and associated structures in Sonora and adjacent areas, México: 1:1,000,000. U.S. Geological Survey, Miscellaneous Field Studies Map 2238.

Stipp, M., Stünitz, H., Heilbronner, R. and Schmid, S. M. (2002). The eastern Tonale fault zone: A 'natural laboratory' for crystal plastic deformation of quartz over a temperature range from 250 to 700 °C. Journal of Structural Geology, 24, 1861-1884.

Valencia-Moreno, M., & Ortega-Rivera, A. (2011). Cretácico Tardío-Eoceno Medio en el noroeste de México-Evolución del arco magmático continental y su contexto geodinámico (orogenia Laramide). In T., Calmus (Eds.), Panorama de la geología de Sonora, México. *Universidad Nacional Autónoma de México, Instituto de Geología, Boletín, 118*, 201–226.

Valencia-Moreno, M., López-Martínez, M., Orozco-Esquivel, T., Ferrari, L., Calmus, T., Noury, M., & Mendívil-Quijada, H. (2021). The Cretaceous-Eocene Mexican Magmatic Arc: Conceptual framework from geochemical and geochronological data of plutonic rocks. *Earth-Science Reviews, 220*, 1–18. 103721. https://doi.org/10.1016/j.earscirev.2021.103721

Valencia-Moreno, M., González-León, C.M., Solari, L., Rascón-Heimpel, M.A., González-Becuar, E., Lozano-Santacruz, R., & Pérez-Arvizu, O., 2024, U-Pb zircón geochronology and geochemistry of the Jurassic magmatic rocks from the region of Cananea and Nacozari, northeastern Sonora, Mexico: timing and composition of the southernmost edge of the Jurassic continental arc. *Canadian Journal of Earth Sciences, 61*, 89–116. https://doi.org/10.1139/cjes-2023-0059

Vázquez Salazar, M. (2018). Geología de las sierras Las Jarillas y El Potrero, región de Santa Ana, norte de Sonora [Bachelor Thesis]. Universidad Estatal de Sonora, Ingeniería en Geociencias.

Vega Granillo, R., Calmus, T. (2003). Mazatan metamorphic core complex (Sonora, Mexico): structures along the detachment fault and its exhumation evolution. *Journal of South American Earth Sciences, 6*, 193-204.

Vermeesch, P., 2012, On the visualisation of detrital age distributions. *Chemical Geology*, 312–313, 190-194, doi: 10.1016/j.chemgeo.2012.04.021

Wernicke, B. (1992). Cenozoic extensional tectonics of the U.S. Cordillera. In B. C., Burchfiel, P. W., Lipman, & M. L., Zoback (Eds.), *The Cordilleran Orogen: Conterminous U.S.* (pp. 553-581). Geological Society of America, The Geology of North America, G-3.

Whitney, D. L., Teyssier, C., Rey, P., Buck, W. R. (2013). Continental and oceanic core complexes. *Geological Society of America Bulletin, 125*, 273–298.

Wong, M. S. & Gans, P. B. (2008). Geologic, structural, and thermochronologic constraints on the tectonic evolution of the Sierra Mazatán core complex, Sonora, Mexico: New insights into metamorphic core complex formation. *Tectonics, 27*, 1–31.

Wong, M. S., Gans, P. B., & Scheier, J. (2010). The $^{40}Ar/^{39}Ar$ thermochronology of core complexes and other basement rocks in Sonora, Mexico: Implications for Cenozoic tectonic evolution of northwestern Mexico. *Journal of Geophysical Research, 115*, 1–19.

Zapata Martínez, J. A., González-León, C. M., Solari, L., & Nourse, J. A. (2018). U-Pb geochronology and geochemistry of Paleocene to Eocene leucocratic plutons of the sierras Magdalena and La Jojoba, northern Sonora, Mexico. *Geological Society of America Abstracts with Programs, 50*(5). doi: 10.1130/abs/2018RM-314307.

FIGURES

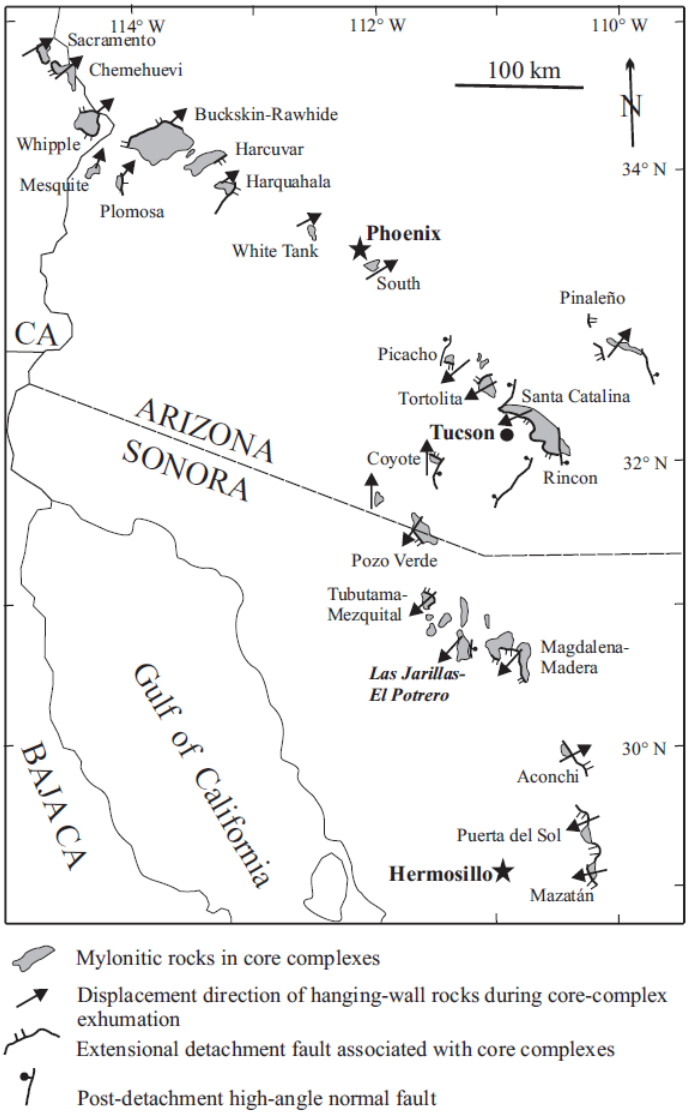

Figure 1. Distribution of the metamorphic core complexes and main associated detachment faults in the region of southeastern California, Arizona and Sonora (modified from Spencer et al., 2019), and location of the Las Jarillas-El Potrero study area (in italics and bold).

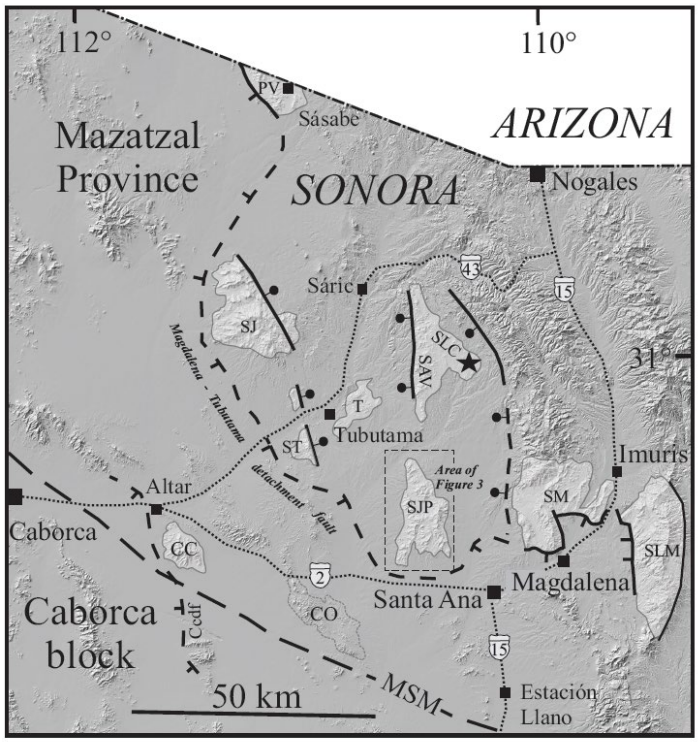

Figure 2. Map of north-central Sonora indicating lower plate areas exposing rocks with mylonitic fabrics of Tertiary metamorphic core complexes (light gray areas), the southwest-vergent Magdalena-Tubutama detachment fault, and the Cerro Carnero detachment fault (Ccdf) (map modified from Nourse et al., 1994; Nourse, 1995). SLM, Sierra La Madera; SM, Sierra Magdalena; SJP, study area of Sierras Las Jarillas-El Potrero; SAV, Sierra El Álamo Viejo; SLC, Sierra Los Chinos; ST, Santa Teresa; T, Tubutama; SJ, San Juan; CC, Cerro Carnero and PV, Pozo Verde. CO, cerros El Ocuca with non-mylonitized strata of the Lower Cretaceous Bisbee Group formations. MSM inferred trace of the Mojave-Sonora megashear. Structural symbols as in Figure 1. The black star indicates location of sample 3-19-19-2, which is one of the two samples dated by $^{40}Ar/^{39}Ar$ thermochronology in this study. Dashed rectangle indicates area of Figure 3.

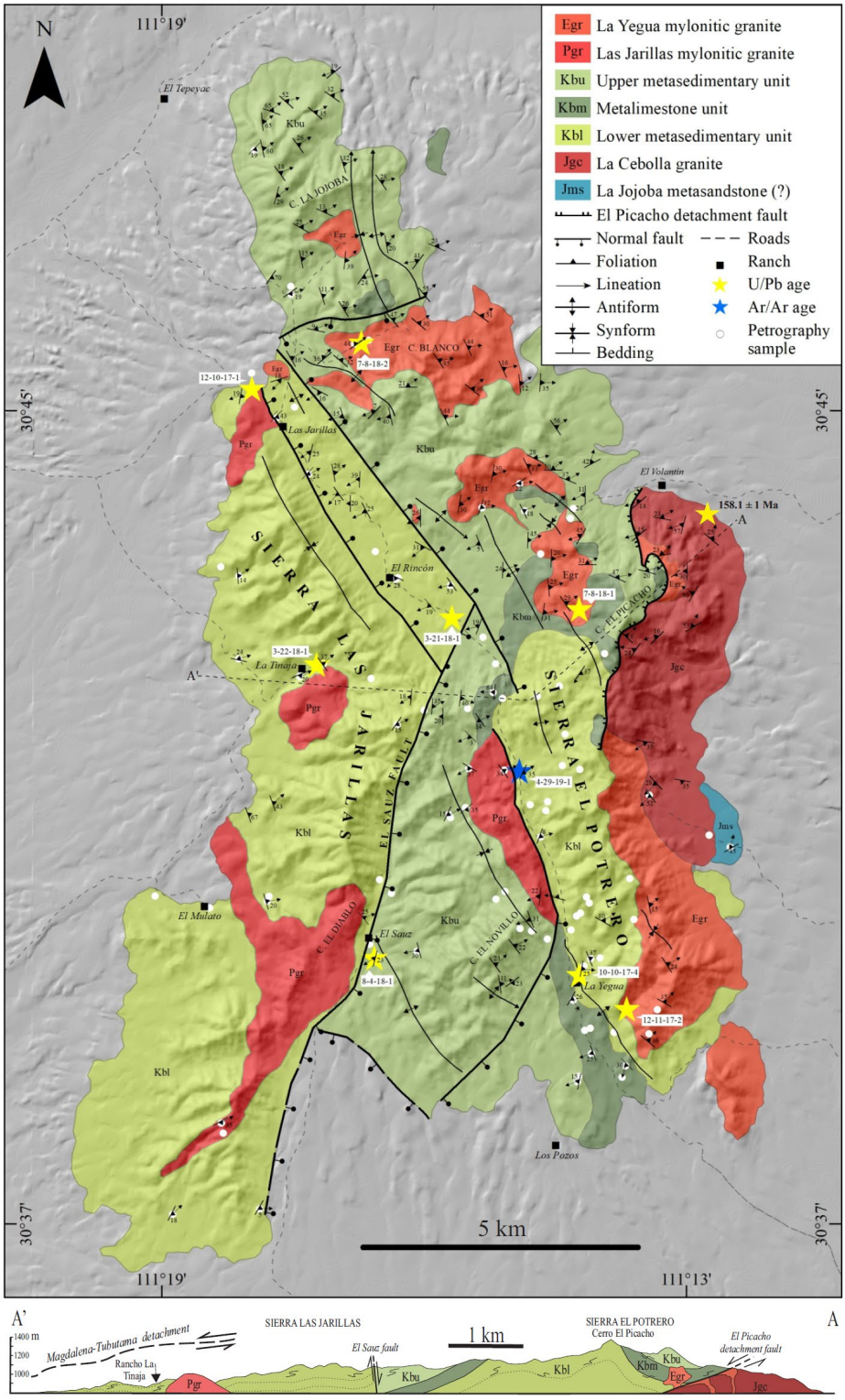

Figure 3. Geologic map of the sierras Las Jarillas-El Potrero, northern Sonora, Mexico with structural section A-A' that schematically shows mesoscale folds with top-to-the-southwest vergence on limbs of map-scale folds, and speculative position of the main Magdalena-Tubutama detachment fault. Location of sample and age reported for the La Cebolla granite by González-León et al. (2017) is shown. Area in grey around the sierras corresponds to recent alluvial sediments.

Figure 4. Photographs of field outcrops. A) Bedded metapelites of the lower metasedimentary unit; B) Metavolcanic bed with glassy texture and contorted flow banding intruded by granitic sills; C) Recrystallized limestone beds of the metalimestone unit. D) outcrop of Cerro El Picacho where the lower metasedimentary unit (Kbl) is overlain by the metalimestone unit (Kbm) that is intruded by the La Yegua mylonitic granite (Egr).

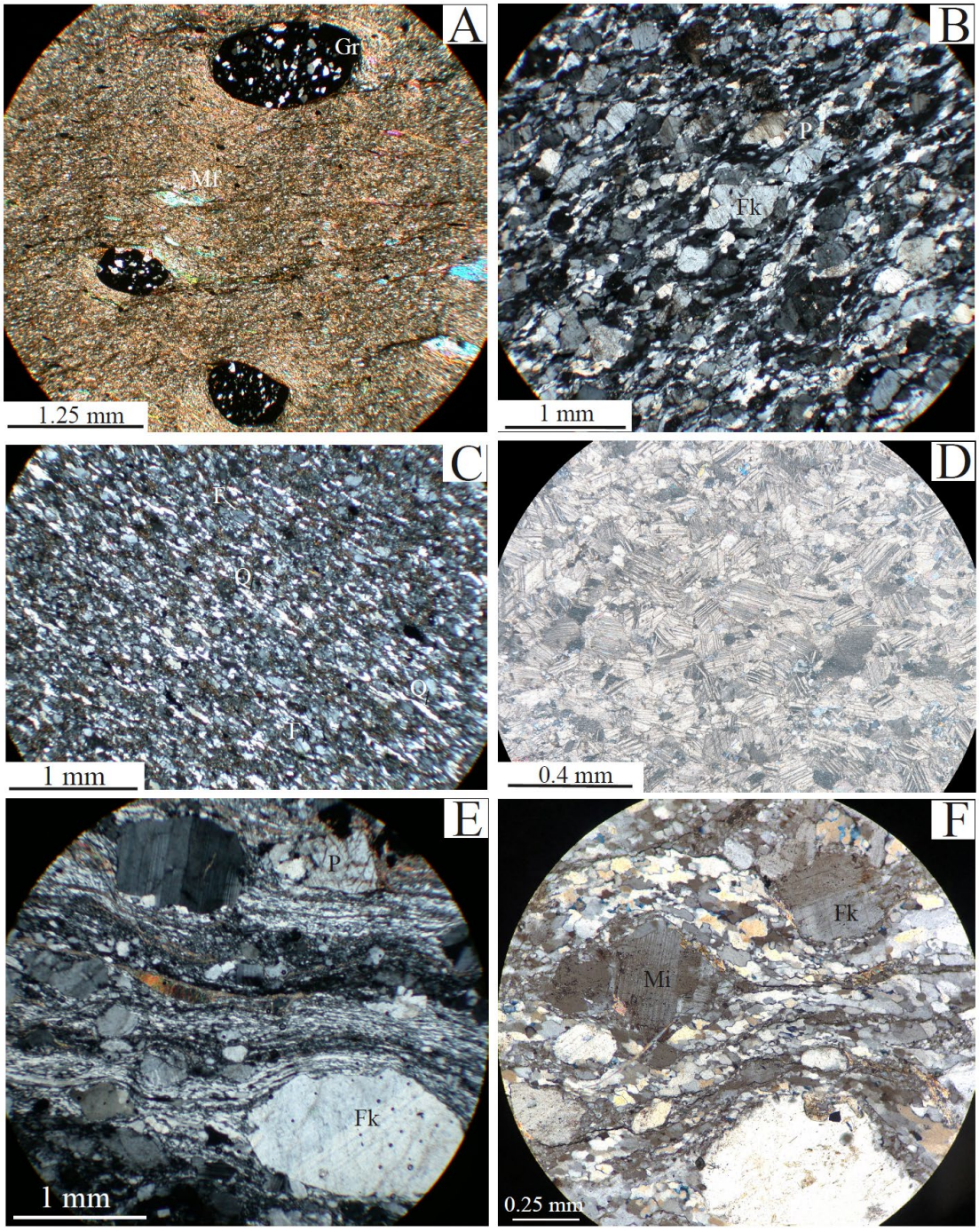

Figure 5. Photomicrographs (polarized light) of representative thin sections of rock samples in the study area. A) Pelitic mica (muscovite ± biotite) schist with subordinate quartz, muscovite mica-fish (Mf) and poikiloblastic garnet (Gr) of sample 1-21-19-5, B) Arkosic metasandstone of sample 7-28-17-4 showing oriented grains of k-feldspar (Fk), plagioclase (P) and bands of recrystallized quartz, C) Fine-grained metavolcanic sample 7-29-17-5 with elongated polycrystalline quartz (Q), subordinate feldspar (F) and dark bands of biotite and <muscovite. D) Recrystallized calcite with polysynthetic twins from sample 7-27-17-1 of the metalimestone unit. E) Sample 3-9-20-2 from Las Jarillas mylonitic granite, and F) sample 3-7-20-2 from La Yegua mylonitic granite with porphyroclasts of k-feldspar (Fk), plagioclase (P) and microcline (Mi).

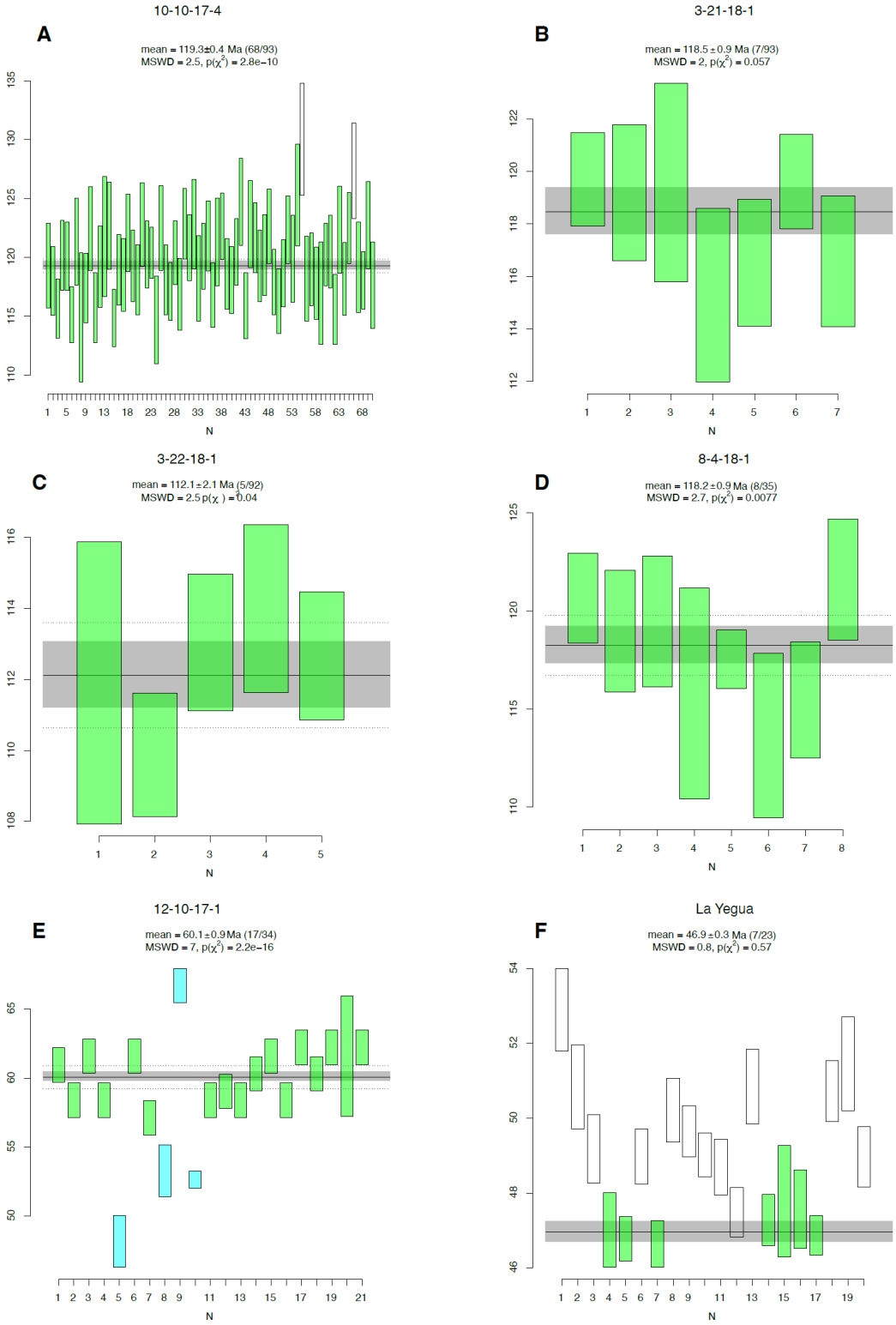

Figure 6. Interpreted $^{206}Pb/^{238}U$ maximum depositional ages for A) metasandstone sample 10-10-17-4 and metavolcanic samples B) 3-21-18-1 and C) 3-22-18-1 from the lower metasedimentary unit, and D) metavolcanic sample 8-4-18-1 from the upper metasedimentary unit. Crystallization mean ages from the mylonitic E) Las Jarillas (sample 12-10-17-1) and F) La Yegua (combined samples 12-11-17-2, 7-8-18-1 and 7-8-18-2) granites.

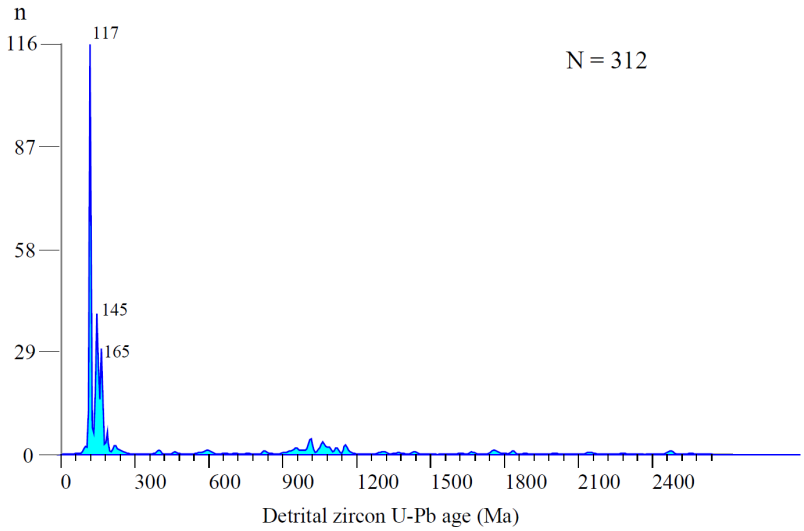

Figure 7. Kernel density estimator plot of the dated zircon grains in samples 10-10-17-4, 3-21-18-1, 3-22-18-1 and 8-4-18-1 showing important Lower Cretaceous and Jurassic ages peaks.

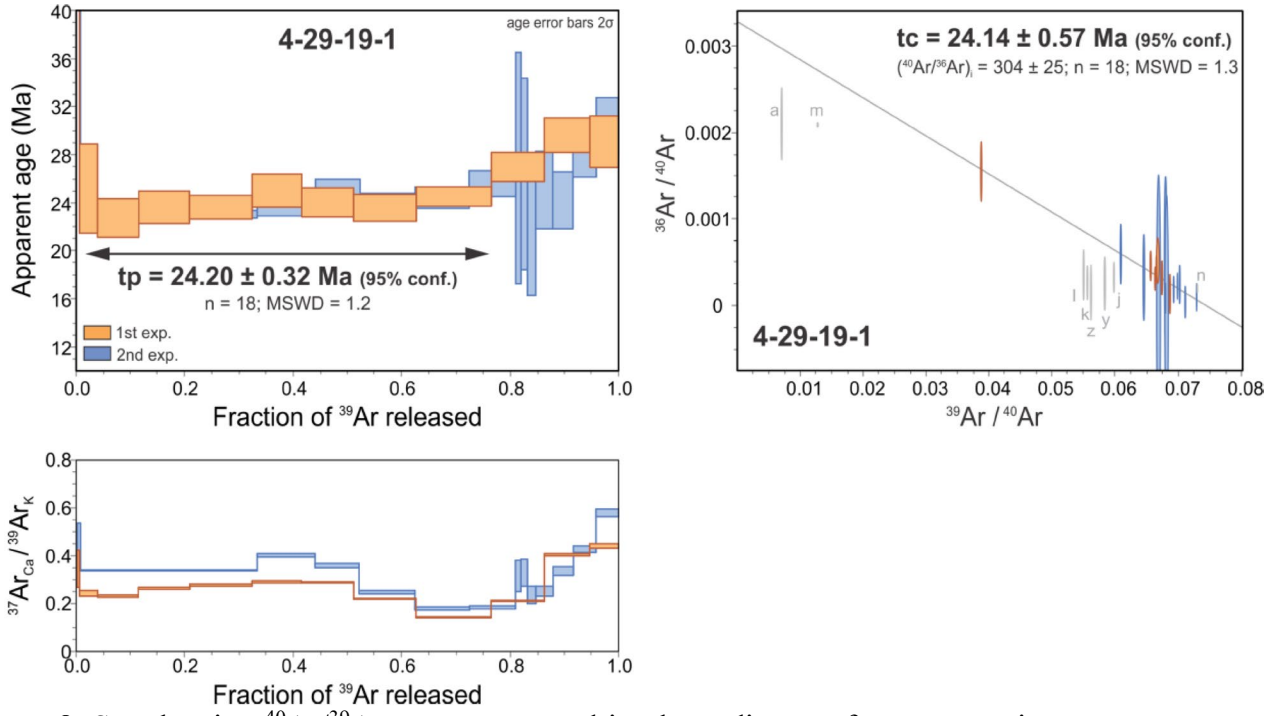

Figure 8. Step-heating $^{40}Ar/^{39}Ar$ age spectra and isochron diagram for a muscovite+quartz concentrate obtained from fine-grained metasandstone sample 4-29-19-1, collected from the lower metasedimentary unit. The plateau and correlation ages are indistinguishable within error. Calculated plateau age (tp), correlation age (tc), and number of steps (n) used in the age calculation are indicated. MSWD: mean squared weighted deviation.

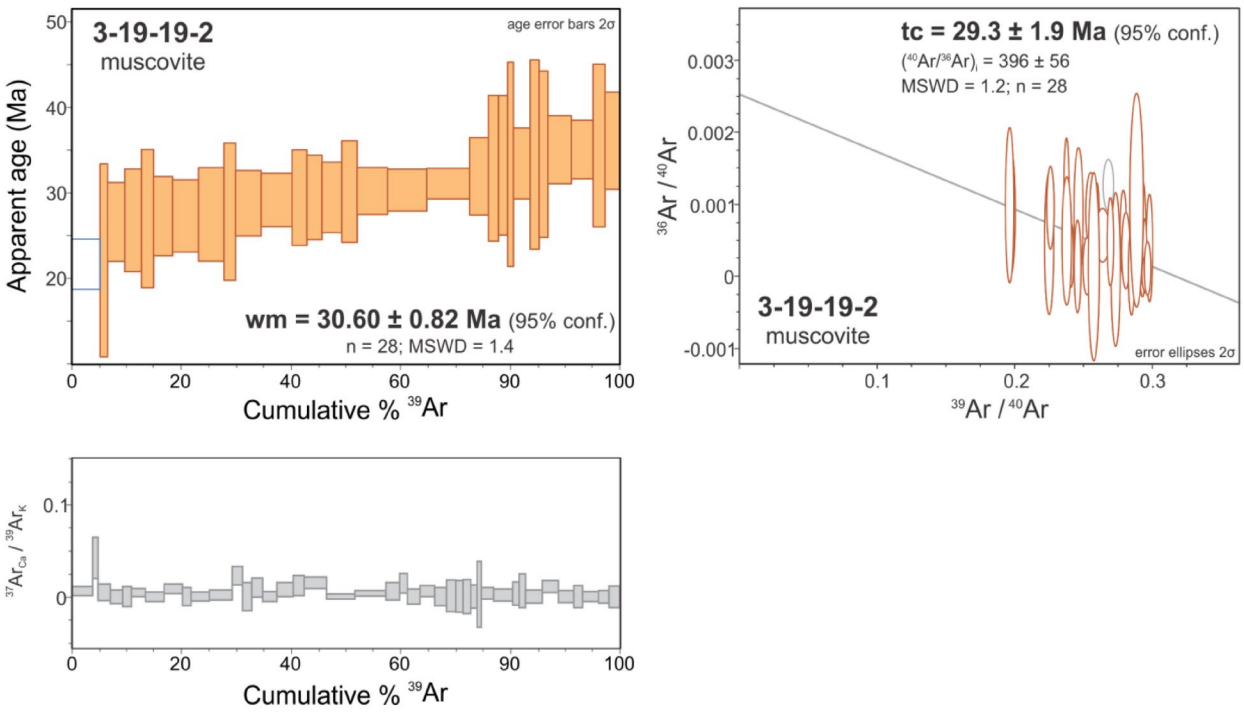

Figure 9. Rank order and isochron diagrams showing $^{40}Ar/^{39}Ar$ total fusion data for muscovite single crystals from mica schist sample 3-19-19-2, collected from the Middle Jurassic Sierra Guacomea rhyolite near Rancho El Joatiqui. Single data are shown with 2σ analytical uncertainty. The calculated weighted mean (wm) and correlation (tc) ages are reported within 95% confidence interval. n: number of steps used in the age calculation; MSWD: mean squared weighted deviation.

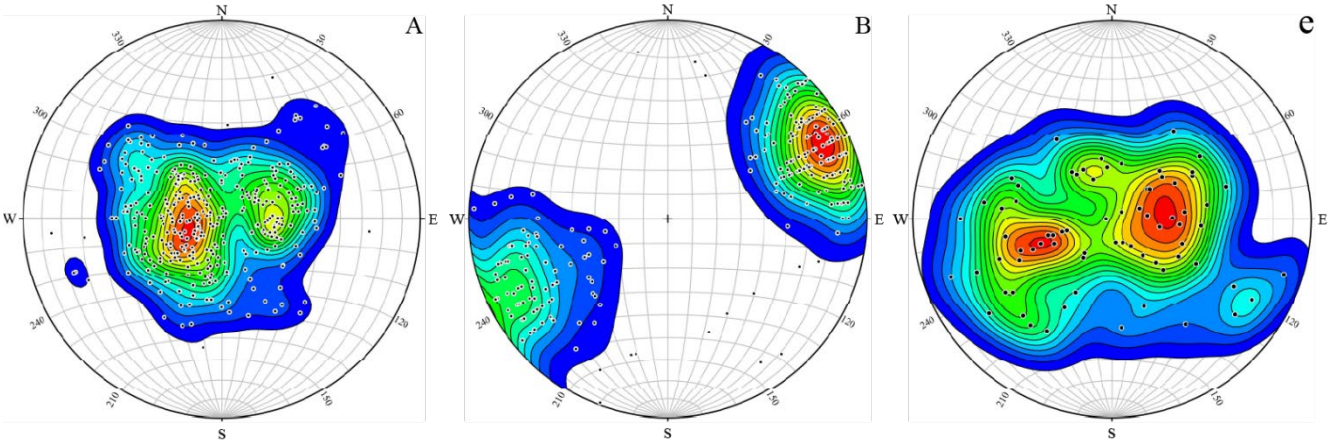

Figure 10. Plots of A) foliation poles (N= 363), B) stretching lineations (N= 242) and C) axial planes (N= 59) from the sierras Las Jarillas-El Potrero. Lower hemisphere equal area projection (Schmidt) produced with Stereonet 10 (Allmendinger, 2019).

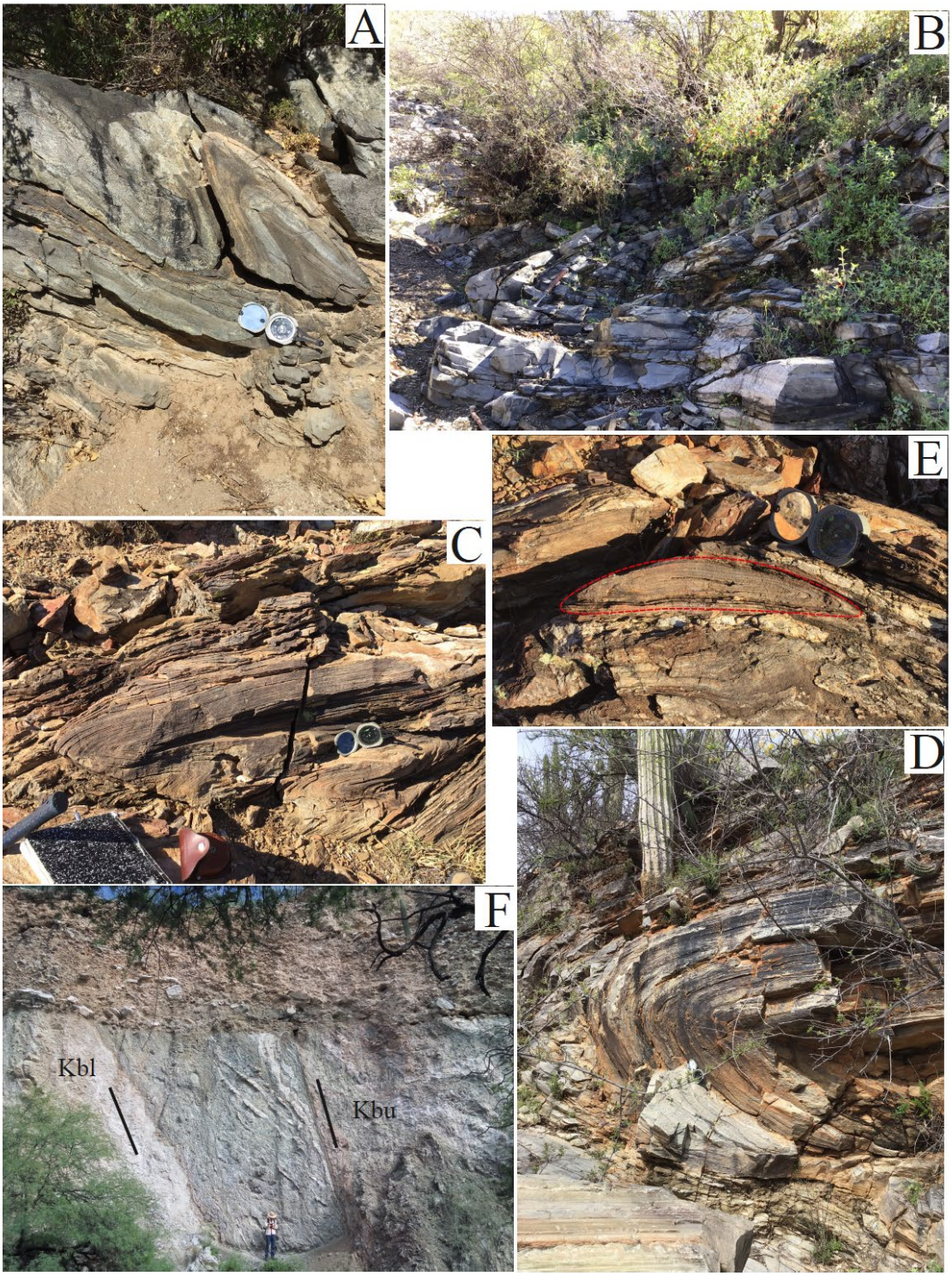

Figure 11. A-D) Outcrop photographs of isoclinal and recumbent folding in metalimestone, metasandstone and metavolcanic rocks. E) Sheath fold in metalimestone. F) El Sauz high-angle normal fault, dipping to the east near rancho El Sauz. The fault and the lower (Kbl) and upper (Kbu) metasedimentary units are covered by recent alluvium conglomerate (person for scale).

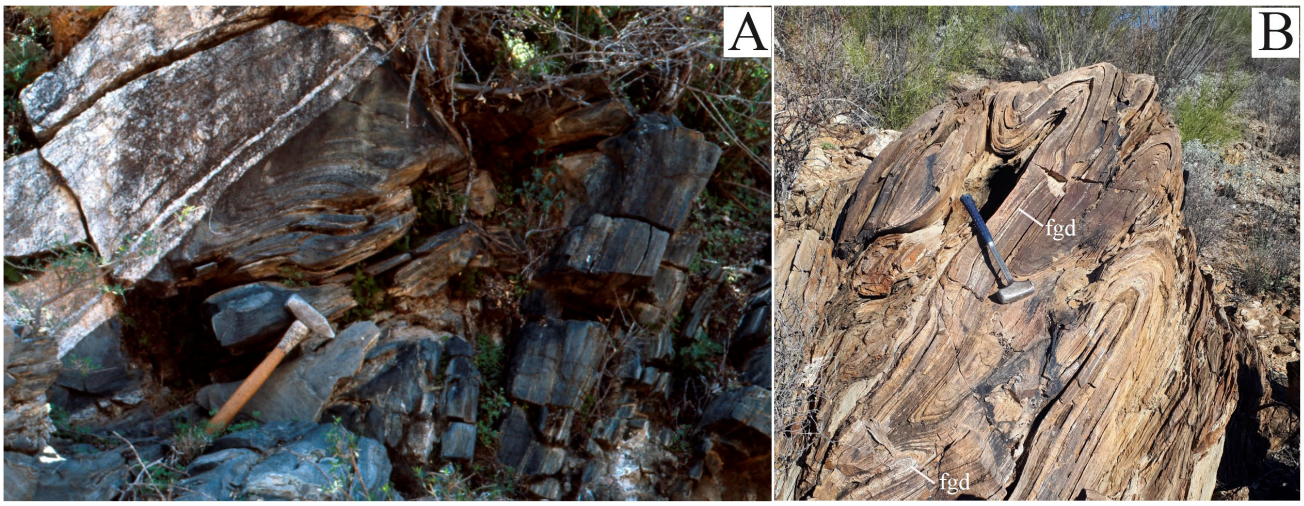

Figure 12. A) Mylonitized pegmatitic dike that cuts folded metasedimentary strata in the southern part of the Sierras Las Jarillas-El Potrero. B) Thin sills (fgd) of leucocratic granite that are folded and boudinaged along metalimestone beds in the southern part of the study area.

TABLES

Table 1. Summary of ages of samples dated in this work from the sierras Las Jarillas-El Potrero

Sample No.	UTM Coordinates (12R) Datum WGS84	Lithology	Unit	Age (Ma)
		$^{206}Pb/^{238}U$ zircon ages		
10-10-17-4	477308; 3391701	Metasandstone	Lower metasedimentary unit	119.3 ± 0.4; MSWD =2.5 (MDA)*
3-21-18-1	475000; 3398184	Metavolcanic	Lower metasedimentary unit	118.5 ± 0.9; MSWD= 2 (MDA)
3-22-18-1	472541; 3397336	Metavolcanic	Lower metasedimentary unit	112.1 ± 2.1; MSWD= 2.5 (MDA)
8-4-18-1	473608; 3392064	Metavolcanic	Upper metasedimentary unit	118.2 ± 0.9; MSWD= 2.7 (MDA)
12-10-17-1	471365; 3402340	Mylonitic granite	Las Jarillas mylonitic granite	60.1 ± 0.9; MSWD= 7 (CA)*
7-8-18-2	473355; 3403176	Mylonitic granite	La Yegua granite	Combined age 46.9 ± 0.3; MSWD= 0.8 (CA)
7-8-18-1	477312; 3398338	Mylonitic granite	La Yegua granite	
12-11-17-2	478174; 3391087	Mylonitic granite	La Yegua granite	
		$^{40}Ar/^{39}Ar$ ages		
4-29-19-1	476224; 3395400	Metasandstone	Lower metasedimentary unit	24.2 ± 0.32 (C-a)*
3-19-19-2	482933; 3428027	Mica schist	Sierra Guacomea rhyolite	30.6 ± 0.82 (C-a)

* MDA = Maximum depositional age
*CA = Crystallization age
*C-a = Cooling age